Analyst

ROYAL SOCIETY OF CHEMISTRY

CRITICAL REVIEW

View Article Online
View Journal | View Issue

Cite this: *Analyst*, 2025, **150**, 4490

Recent advances and applications of electrochemical mass spectrometry for real-time monitoring of electrochemical reactions

Xuemeng Zhang,[a,b] Yiteng Zhang,[a] Baozhen Yuan[a] and Qianhao Min *[a]

Real-time monitoring of electrochemical reactions is crucial for advancing energy conversion and storage, electrocatalysis, organic electrosynthesis, and electroanalysis. Despite progress in *in situ* spectroscopic and electrochemical techniques, these methods fail to directly resolve and track multiple electrogenerated species simultaneously during electrochemical processes. Electrochemical mass spectrometry (EC-MS) bridges this gap by providing direct molecular-level compositional and structural information while simultaneously monitoring the evolution of newborn species at the electrode–electrolyte interfaces (EEIs). Propelled by the ongoing improvements in ionization sources and electrochemical cells, EC-MS methods have broadened the functional scope from online detection of reaction products to the rapid capture of fleeting intermediates and, most recently, to simultaneous real-time tracking of the dynamics of multiple intermediates. This progressive advancement establishes EC-MS as a robust methodology for mechanistic investigation of electrochemical reactions. This review focuses on the recent advances in EC-MS methods and their applications in exploring organic electrosynthesis, electrocatalysis, lithium-ion batteries (LIBs) and electrochemiluminescence (ECL). Finally, we outline the current limitations and future directions for EC-MS technology, forecasting its expanding utility in electrochemical reaction monitoring.

Received 25th July 2025,
Accepted 7th September 2025

DOI: 10.1039/d5an00785b

rsc.li/analyst

1. Introduction

Electrochemical reactions, involving electron transfer at the electrode–electrolyte interfaces (EEIs), form the cornerstone of sustainable energy systems, selective electrosynthesis, and electrocatalyst design.[1–3] Real-time monitoring of electrochemical processes is paramount for mapping intricate reaction pathways and elucidating the underlying reaction mechanisms.[4,5] Due to the insufficient temporal resolution, offline analytical techniques based on spectroscopy or mass spectrometry fail to describe chemical transformations at the EEIs in real time.[6,7] Conventional electrochemical methods track electron-transfer behaviors at EEIs by correlating current

[a]*State Key Laboratory of Analytical Chemistry for Life Science, Chemistry and Biomedicine Innovation Center, School of Chemistry and Chemical Engineering, Nanjing University, Nanjing 210023, P. R. China*
[b]*Shenzhen Research Institute of Nanjing University, Shenzhen 518057, P. R. China*

Xuemeng Zhang

Xuemeng Zhang is currently a postdoctoral fellow at Nanjing University. She received her Ph. D. degree majoring in analytical chemistry from Nanjing University, China, in 2022. Her research focuses on the development of ambient ionization mass spectrometry techniques for the bioanalysis and dynamic monitoring of chemical and electrochemical reactions.

Yiteng Zhang

Yiteng Zhang obtained his Master's degree in analytical chemistry from Nanjing University. He is currently a Ph. D. student in chemistry at Rice University, with research interests in mass spectrometry and bioimaging.

with the applied potential or time, yet inherently lack molecular-level insights into electrochemical processes.[8,9] Recently, researchers have developed *in situ* spectroscopic methods (*e.g.*, *in situ* electron paramagnetic resonance (EPR),[10,11] *in situ* Raman[12,13] and *in situ* FTIR[14,15]) to acquire real-time spectral fingerprints of newborn species at the electrode interface, facilitating the *in situ* characterization and dynamic tracking of reaction intermediates. Despite this progress, these methodologies still cannot directly reveal the intrinsic composition and structure of compounds in electrochemical reactions and face challenges in real-time identification of multiple short-lived intermediates during dynamic electrochemical processes, thereby presenting notable technical limitations in elucidating electrochemical reaction mechanisms at the molecular level.

Mass spectrometry (MS) excels at providing direct molecular-level compositional and structural information for multiple analytes with high sensitivity and specificity.[16,17] By utilizing this merit, electrochemical mass spectrometry (EC-MS) has been developed for direct acquisition of molecular information and real-time monitoring of intermediates and products during electrochemical processes, serving as an ideal tool for mechanistic investigation of electrochemical reactions.[18–20] The pioneering application of MS for the online detection of electrochemical reaction products was reported by Bruckenstein *et al.* in 1971.[21] In this work, an electrochemical cell containing porous electrodes was coupled with electron impact ionization mass spectrometry (EI-MS) to analyse gaseous and volatile products, thereby establishing the foundation for real-time monitoring of electrochemical reactions. Building upon this work, differential electrochemical mass spectrometry (DEMS) was developed by Wolter and Heitbaum in 1984 and has since become a classic technique for online detection of gaseous species in electrochemical reactions.[22] For liquid species, the combination of electrochemical flow cells with electrospray ionization mass spectrometry (ESI-MS) provides an efficient means for real-time monitoring of liquid products during electrochemical processes.[23,24] To further achieve the rapid capture of fleeting intermediates, integrating an electrochemical cell into an electrospray ion source has proved to be an effective strategy to shorten the transfer distance from the EEIs to the MS inlet.[18,25]

Furthermore, with the unique advantage of the *in situ* analysis of newborn species at the electrode interface, the ambient ionization mass spectrometry (AIMS) proposed by Cooks' group facilitates the real-time readout of molecular information and detection of short-lived intermediates from interfacial electrochemical processes, providing an important theoretical basis for the study of electrochemical reaction mechanisms.[26,27] Recently, driven by the critical importance of tracking the dynamic fate of intermediates for investigating electrochemical reaction mechanisms, researchers have turned their attention to developing EC-MS with both excellent temporal and potential resolutions, aiming to comprehensively crack reaction networks under *operando* conditions.[28]

In this review, we will conduct a comprehensive and systematic overview of the evolution of EC-MS methods tailored to specific research objectives, focusing on the online detection of electrochemical reaction products, rapid capture of fleeting intermediates, and real-time tracking of intermediate dynamics (Fig. 1). The technical implementations of existing EC-MS platforms are subsequently summarized in terms of their specialized design, including electrochemical cell design, ionization techniques, and interface configurations. Furthermore, we delve into detailed discussions of EC-MS applications in organic electrosynthesis, electrocatalysis, lithium-ion batteries (LIBs), and electrochemiluminescence (ECL). Finally, we also outline the current scope and future directions for the design and improvement of EC-MS technology and anticipate its expanding utility in electrochemical reaction monitoring.

2. Development of EC-MS methods for real-time monitoring of electrochemical processes

2.1 EC-MS methods for online detection of reaction products

Online monitoring and accurate identification of electrochemical transformation products including both the desired

Baozhen Yuan

Baozhen Yuan is a Ph.D. student in the School of Chemistry and Chemical Engineering at Nanjing University. Her research focuses on the development of electrochemical mass spectrometry methods for mechanistic studies on the electrocatalytic CO_2 reduction reaction (CO_2RR).

Qianhao Min

Qianhao Min received his B.S. (2007) and Ph.D. (2012) degrees in chemistry from Nanjing University. After working as a visiting scholar at Stanford University, he joined the faculty of Nanjing University as an associate professor in 2015 and was further promoted to full professor in 2022. His research focuses on operando mass spectrometry and mass tagging-based mass spectrometry for dynamic monitoring of molecular events in chemical and biological processes.

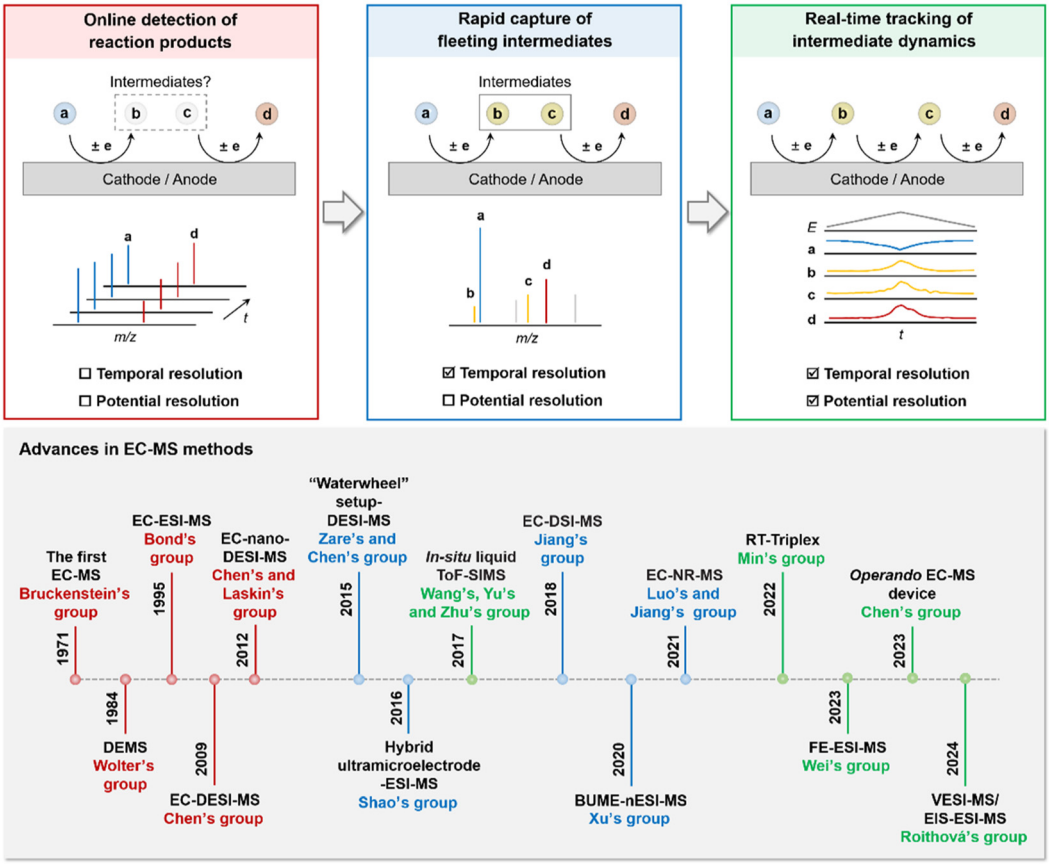

Fig. 1 The progression and historical trajectory of electrochemical mass spectrometry (EC-MS) for real-time monitoring of electrochemical processes.

analytes and unintended by-products are of paramount guiding significance for the development of organic electrosynthesis methodologies, design of electrochemical catalysts and fabrication of energy storage devices.[29] With high sensitivity and selectivity, MS simultaneously obtains molecular information from multiple targets, while tandem MS facilitates structural elucidation, offering an ideal means to detect these products in complex reaction systems. Coupling electrochemical cells with MS is capable of accurate and real-time characterization of electrochemical transformation products through precise mass-to-charge ratios (m/z) and immediate feedback.[30,31] Among numerous EC-MS methods, DEMS, which comprises an electrochemical cell, a sample inlet interface and a mass spectrometer, offers an *operando* and cost-effective tool to monitor the evolution of gaseous and volatile products during electrochemical processes.[21,32] In DEMS, a membrane inlet interface is constructed to effectively separate the electrolyte solution from the vacuum environment, making it a more popular approach within the emerging energy conversion and storage systems (Fig. 2a).[33] During DEMS detection, gaseous and volatile species generated at the electrode diffuse through a 50–100-μm thick electrolyte layer and subsequently pass through a Teflon membrane to reach the mass spectrometer.[34] Bell's group presented a novel DEMS setup that allowed for the real-time quantification of ion signal intensities of volatile reaction products. To demonstrate this capability, they used the electrochemical CO_2 reduction reaction (CO_2RR) on polycrystalline copper as a model reaction to quantify products in real time at different potentials.[35] To further overcome the limitation of conventional DEMS methods sampling only bulk electrolyte products, this group used a modified DEMS with a catalytically coated pervaporation membrane to directly sample the interface, measuring CO_2 and reaction products in the hydrogen evolution reaction (HER) and the CO_2RR on silver and copper electrodes.[36] Recently, Hasa *et al.* developed a flow electrolyzer mass spectrometry (FEMS) system by integrating a flow cell with a gas diffusion electrode (GDE) into the DEMS technique. In this setup, the probe was positioned in close proximity to the electrode surface, enabling real-time detection of species generated directly from the catalyst layer (Fig. 2b). To illustrate this point, they examined the electrochemical carbon monoxide reduction reaction (CORR) on polycrystalline copper, revealing the oxygen incorporation mechanism in acetaldehyde.[37] With the ability to monitor gaseous products in real time, DEMS contributes to correlating various reaction products with time or potential.[38] Cao *et al.* integrated DEMS with gas chromatography (GC) to quantify gas release from the decomposition of

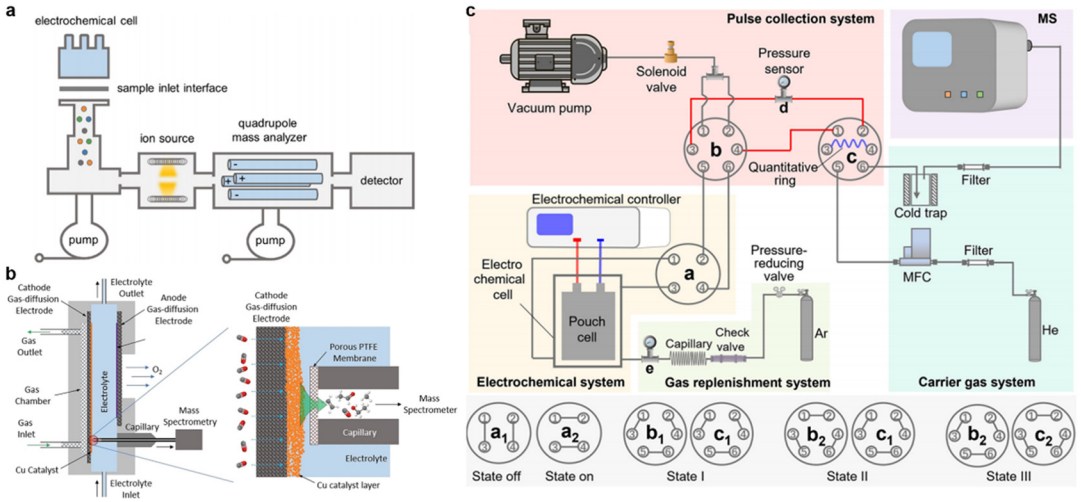

Fig. 2 (a) Structure and composition of the DEMS setup. Reprinted with permission from ref. 33. Copyright (2024) The Royal Society of Chemistry. (b) Schematic illustration of the GDE design of flow electrolyzer MS. Reprinted with permission from ref. 37. Copyright (2021) Wiley-VCH. (c) Design and construction of the *operando* pulse EC-MS (p-EC-MS) system. Reprinted with permission from ref. 41. Copyright (2024) American Chemical Society.

Li_2CO_3 and carbon electrodes in LIBs and have identified that singlet oxygen ($^1O_2$) as the primary reactive species attacks the carbon substrate and electrolytes, leading to the formation of CO_2 and CO as gaseous side products.[39] Chen *et al.* coupled DEMS with distribution of relaxation times (DRT) analysis to differentiate the contributions of charge-transfer limited Li_2O_2 and surface-passivation dominated Li_2CO_3 to overpotential growth during Li–O_2 battery charging.[40] Facing the limitation that current DEMS cannot monitor industrial-scale LIBs in real time, Peng's group developed an *operando* pulse EC-MS (p-EC-MS) featuring a specialized electrochemical cell, a programmed inlet, and a gas replenishment system for the non-destructive and long-term gas analysis of practical lithium-ion pouch batteries (Fig. 2c).[41]

While DEMS has been extensively employed for the sensitive and real-time detection of gaseous products or volatile species during electrochemical processes, a comprehensive understanding of reaction pathways often requires the simultaneous acquisition of information about liquid-phase products as well. Owing to the high ionization efficiency, ESI-MS has established itself as a commonly used soft ionization source for the analysis of liquid-phase species.[42] Recognizing its potential, researchers have developed online EC-ESI-MS by direct coupling of an electrochemical flow cell with ESI-MS, in which the liquid products are continuously pumped into the MS inlet through a capillary tube. By establishing this effective connection, the oxidative phase I metabolism of the mycotoxins citrinin (CIT) and dihydroergocristine (DHEC) was simulated by electrooxidation reactions, and the products were detected in real time.[43] Chen's group developed electrochemical ionization mass spectrometry (ECI-MS) to directly characterize alloys at the molecular level without the need for tedious sample pretreatment.[44] As shown in Fig. 3a, bulk alloys were electrolyzed to form metal ions, which were then online chelated with specific ligands and subsequently detected using ESI-MS. The high surface-to-volume ratios of electrochemical microreactors, coupled with their ability to allow very precise control over reaction parameters like temperature, residence time, flow rate, and pressure, make them highly suitable for direct coupling with ESI-MS.[45,46] Van den Brink *et al.* presented a drug screening method using an electrochemical microchip coupled with ESI-MS to generate phase I and phase II drug metabolites and to demonstrate protein modification by reactive metabolites.[47] Herl *et al.* coupled bare screen-printed carbon electrodes (SPCEs) with ESI-MS, enabling real-time characterization of the redox properties of thymine (Fig. 3b). Their results have shown that dimeric species are the main products formed upon electrochemical oxidation.[48]

By conducting both batch and rapid screening of electrochemical synthesis products, high-throughput experimentation (HTE) demonstrates considerable potential to revolutionize electrosynthesis, offering a pathway to significantly faster and more efficient synthetic development.[16,49,50] Wan *et al.* established a picomole-scale real-time electrooxidation screening platform based on nanoelectrospray ionization mass spectrometry (nESI-MS), ingeniously utilizing the ion emitter as both the reactor and the ionization source to enable rapid and high-throughput analysis of products in organic electrosynthesis reactions.[51] Recently, Baker's group reported a new high-throughput electrochemistry platform, colloquially called "Legion", consisting of 96 independently controlled electrochemical cells compatible with standard 96-well plates for applications in electroanalysis and electrosynthesis.[52] Collaborating with this group, Yan's group developed a high-throughput screening platform by interfacing this "Legion" arrayed electrochemistry and nESI-MS for rapid screening and quantitation of electrosynthetic products (Fig. 3c).[53] For most electrocatalytic systems that generate both gaseous and liquid-phase products (like the CO_2RR), real-time monitoring of these products is critical for understanding catalytic performance

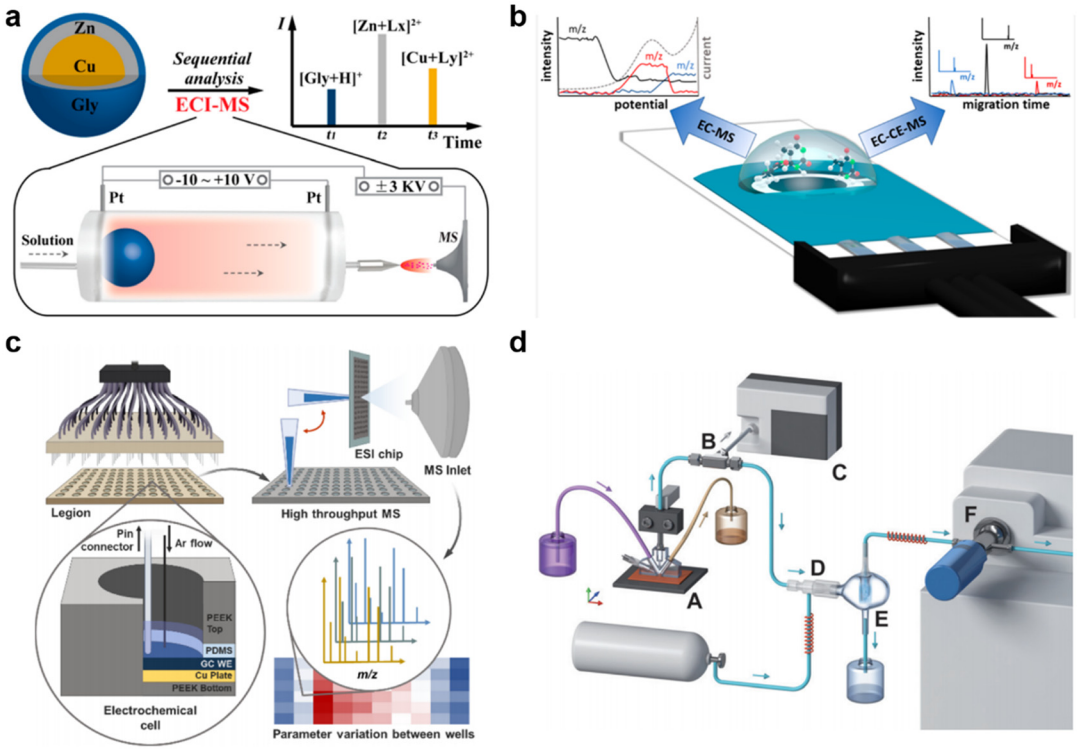

Fig. 3 (a) Schematic illustration of the electrochemical ionization mass spectrometry (ECI-MS) method for analysis of alloys. Reprinted with permission from ref. 44. Copyright (2018) American Chemical Society. (b) Schematic of the EC-MS setup integrating screen-printed carbon electrodes (SPCEs) and ESI-MS. Reprinted with permission from ref. 48. Copyright (2020) American Chemical Society. (c) Workflow of Legion-MS for high-throughput electrochemistry experiments. Reprinted with permission from ref. 53. Copyright (2024) American Chemical Society. (d) Schematic of electrochemical real-time mass spectrometry (EC-RTMS). Reprinted with permission from ref. 54. Copyright (2019) Wiley-VCH.

over extended reactor operation. However, reports of EC-MS techniques capable of real-time, simultaneous monitoring of both gaseous and liquid phases remain scarce. For this reason, Khanipour *et al.* introduced an electrochemical real-time mass spectrometry (EC-RTMS) approach that enables concurrent detection of gaseous and liquid products during the electrochemical CO_2RR.[54] As illustrated in Fig. 3d, the electrolyte and electrochemical products from the electrochemical flow cell are separated into gas and liquid streams *via* a phase separator. Then, the gaseous products pass through a hydrophobic membrane and are subsequently detected using an electron ionization quadrupole mass spectrometer (EI-QMS), while the degassed electrolyte is nebulized and observed using direct analysis with a real time mass spectrometer (DART-MS). This method facilitates real-time tracking of both gas- and liquid-phase products, providing valuable insights for guiding the design of durable and selective catalysts under realistic electrochemical operating conditions, which opens up exciting prospects for guiding the design of new, robust catalysts tailored for selective electrosynthesis under dynamic conditions.

2.2 EC-MS methods for rapid capture of fleeting reaction intermediates

Reaction intermediates play essential roles in electrochemical reactions, which are highly desirable for governing the reaction pathway, determining the kinetic rate, and dictating product selectivity.[55,56] Consequently, rapid capture of these reaction intermediates provides deep insights for elucidating reaction mechanisms and optimizing electrochemical systems.[57,58] However, the rapid transfer of short-lived intermediates from the EEIs to the gas phase for mass spectrometric detection within a sufficiently short timeframe remains a critical challenge in current EC-MS technology. To address this limitation, the most common strategy is to minimize the electrode-to-MS inlet distance, thereby enabling the rapid capture and characterization of transient species. Among them, AIMS technologies, pioneered by Cooks' group, capitalize on their unique capacity for direct extraction of analytes from surfaces with minimal or no sample pretreatment.[26] As a foundational AIMS technique, desorption electrospray ionization mass spectrometry (DESI-MS) enables rapid transfer of newborn species at the EEIs into the MS inlet *via* charged droplets, offering unique advantages for *in situ* analysis of electrogenerated species.[59] By directly coupling DESI-MS with an electrochemical cell using an edge plane graphite as a working electrode (WE) (Fig. 4a), Brownell *et al.* successfully captured multiple key intermediates during alcohol electrooxidation.[60] Zare's group created an EC-MS device based on a "waterwheel" WE capable of rapid, *in situ* analysis of electrochemical species within sub-millisecond timescales.[19,20] As shown in Fig. 4b,

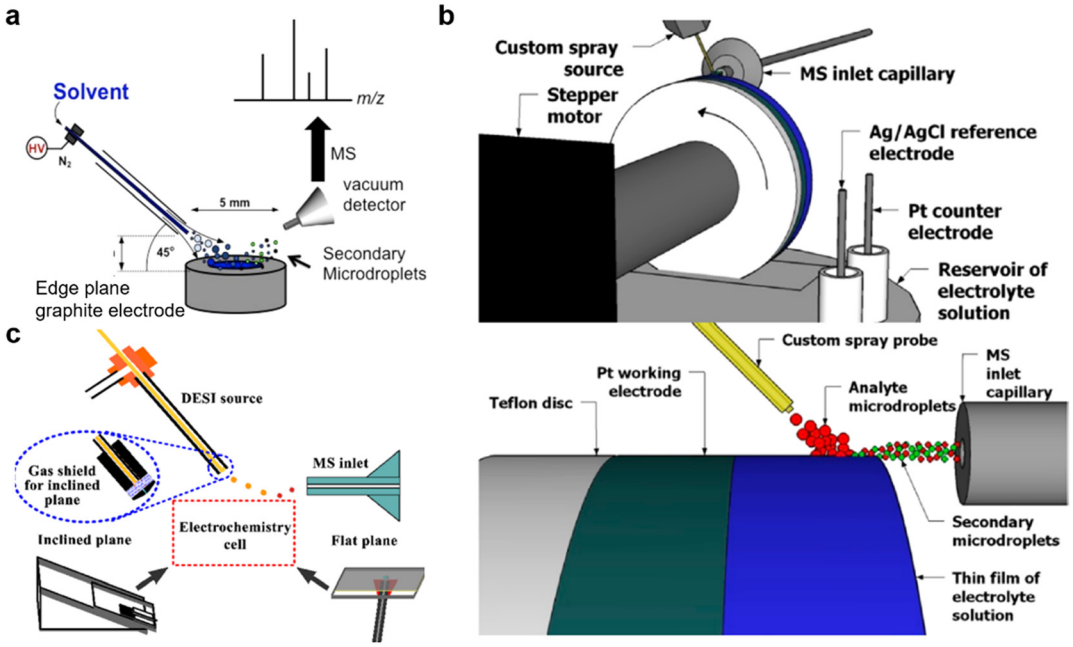

Fig. 4 (a) Schematic illustration of EC-DESI-MS employing edge plane graphite as the working electrode (WE). Reprinted with permission from ref. 60. Copyright (2013) American Chemical Society. (b) Structure and composition of EC-DESI-MS using a rotating waterwheel as the WE. Reprinted with permission from ref. 19. Copyright (2015) American Chemical Society. (c) Schematic of the EC-DESI-MS platform featuring conductive carbon paper WE. Reprinted with permission from ref. 61. Copyright (2017) American Chemical Society.

this EC-DESI-MS platform employs a platinum disc WE partially submerged in an electrolyte, alongside a counter electrode (CE) and Ag/AgCl reference electrodes (RE). The minimal distance (2 mm) between the WE and the MS inlet allows for the detection of transient diimine intermediates formed during the electrochemical oxidation of uric acid and xanthine. Following this idea, their group further developed an EC-DESI-MS platform featuring a conductive carbon paper WE (Fig. 4c). By implementing both grooved-slope and smooth-planar configurations, this system successfully detected nitrenium ions in the electrooxidation reaction of 4,4′-dimethyoxydiphenylamine (DMDPA) and di-*p*-tolylamine (DPTA).[61]

Furthermore, integrating the electrochemical cell into an ESI emitter also significantly reduces the transfer time of newborn species from the EEIs to the MS inlet, making it easier to identify fleeting intermediates. Jiang's group developed droplet spray ionization mass spectrometry (DSI-MS) by mounting a three-electrode system at one corner of the glass slide, enabling real-time detection of aniline (ANI) radical cations and *N*,*N*-dimethylaniline (DMA) radical cations during the electrochemical polymerization of ANI and electrooxidation of DMA.[62] In this EC-MS setup, voltages of 4.5 kV + ΔE and 4.5 kV were applied to the WE and CE, respectively, in which 4.5 kV acted as the droplet spray voltage, while ΔE was the electrooxidation potential driving the electrochemical reaction (Fig. 5a).[63] Wei's group established a floating electrolytic electrospray ionization platform (FE-ESI-MS) for *in situ* electrochemical process monitoring and intermediate characterization.[64] As shown in Fig. 5b, by integrating a micro electrolytic cell into the nESI and controlling the polarity of voltage (ΔV), this design decoupled electrolysis from electrospray, overcoming limitations of conventional ESI and allowing investigation of any electrochemical process across oxidative or reductive modes in both positive and negative polarities. By inserting a Pt wire into a large-orifice (139 μm) quartz capillary (Fig. 5c), Yan's group created a unique microreactor environment at the solution–air interface of the resulting Taylor cone. This setup allows for continuous electrode–reactant contact and accelerates electrochemical reactions within the confined volume.[25,65] Using the porous structure of nitric acid-treated carbon fiber paper (A-CFP) as the ESI emitter and WE permitted shorter ion transport distances and a larger sample contact area in the EC-MS setup, therefore achieving the real-time monitoring of electrochemical reaction intermediates, such as chlorpromazine (CPZ), 1,4-diazabicyclo octane (DABCO), and *N*-phenyl-1,2,3,4-tetrahydroisoquinoline (*N*-Ph-THIQ) radical cations on the millisecond scale (Fig. 5d).[66] Similarly based on carbon paper electrodes, Zhang's group developed a novel "paper-in-tip" platform integrating a triangular conductive paper within a plastic pipette tip to function simultaneously as an electrospray emitter and a bipolar electrode (BPE) (Fig. 5e) and achieved the synchronized electrospray ionization and bipolar electrolysis upon application of a single high voltage.[67] Bipolar electrolysis facilitates complementary oxidation and reduction reactions independent of MS ion mode polarity, providing structural insights into mechanism elucidation.

Based on the above research studies, the strategy of directly constructing an ultramicroelectrode at the tip of the ion

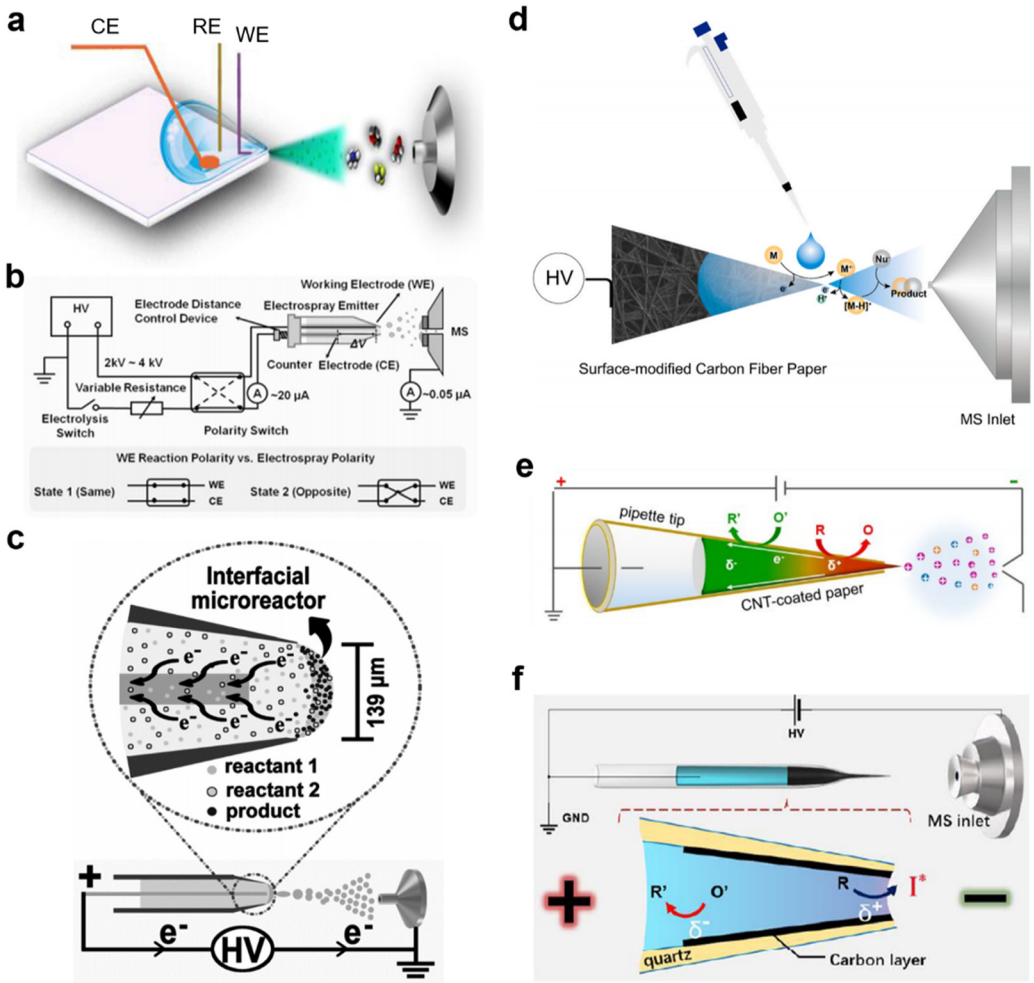

Fig. 5 (a) Schematic illustration of droplet spray ionization mass spectrometry (DSI-MS). Reprinted with permission from ref. 62. Copyright (2018) American Chemical Society. (b) Schematic of the floating electrolytic electrospray ionization platform (FE-ESI-MS). Reprinted with permission from ref. 64. Copyright (2023) Wiley-VCH. (c) Schematic of the interfacial microreactor for accelerating electrochemical reactions in nESI-MS. Reprinted with permission from ref. 25. Copyright (2020) Wiley-VCH. (d) Schematic of the EC-MS setup based on acid-treated carbon fiber paper (A-CFP). Reprinted with permission from ref. 66. Copyright (2023) Elsevier. (e) Schematic of paper-in-tip bipolar electrospray MS. Reprinted with permission from ref. 67. Copyright (2024) Wiley-VCH. (f) Schematic of the EC-MS platform coupling carbon bipolar electrode (BPE) with nESI-MS. Reprinted with permission from ref. 70. Copyright (2020) Wiley-VCH.

emitter in the electrospray ion source not only shortens the distance between the EEIs and the MS inlet but also increases the electrode-surface-to-volume ratio, thereby fostering the capture of transient intermediates during electrochemical processes. Shao's group fabricated a hybrid ultramicroelectrode by introducing a carbon microelectrode, agar-gel/organic hybrid ultramicroelectrodes or water/PVC-gel hybrid ultramicroelectrodes into the tip of a quartz theta micropipette.[68,69] Driven by a piezoelectric pistol, this hybrid ultramicroelectrode serves both as an electrode and an nESI emitter for MS, thereby simultaneously initiating electrochemical reactions and enabling rapid capture of reaction intermediates. Xu's group coupled a carbon BPE with nESI-MS for the online monitoring of ultrafast electrochemical processes (Fig. 5f).[70] Using this technique, the researchers detected, for the first time, the tripropylamine (TPrA) radical cation with a half-life of 200 μs and the catechol quinone radical, thereby revealing the electrochemical oxidation mechanisms of TPrA and dopamine at the molecular level. In addition, they further fabricated a gold microelectrode into the tip of an ion emitter and successfully realized the low-delay combination of electrochemistry and MS.[71] Leveraging the rapid response of this coupling interface, the fleeting intermediates formed from the electrooxidation of carbazoles and indoles were unambiguously detected. Despite boosting temporal resolution of EC-MS through direct integration of electrodes and ESI, inherent in-source electrochemical reactions during the electrospray process distort intentional electrode processes, making true electrochemical system reconstruction unattainable. For this reason, Pradeep's group presented a novel EC-MS coupling setup by employing a paper-based electrochemical cell supported by carbon nanotubes (CNTs). In this setup, ions

formed electrochemically at appropriate potentials were efficiently ejected into the gas phase from the CNT-modified paper, eliminating the requirement for an additional potential to achieve ion transfer.[72]

2.3 EC-MS methods for real-time tracking of the intermediate dynamics

Conventional electrochemical techniques, such as cyclic voltammetry (CV) and chronoamperometry (CA), enable the dynamic evaluation of reaction thermodynamics and quantitative interrogation of interfacial kinetics *via* applied potential or time-dependent current measurements.[73] However, these methods lack the capability to simultaneously follow the molecular-level dynamics of multiple reaction intermediates in dynamic electrochemical processes. This highlights the need for an advanced EC-MS platform that excels in both temporal resolution and the dynamic monitoring of the potential- and time-dependent fates of multiple intermediates, which is poised to enable the comprehensive understanding of the reaction mechanism and the elucidation of interactions between reactive intermediates within intricate electrochemical reaction networks. Recent efforts in coupling voltammetry methods with MS have demonstrated significant mechanistic insights. Roithová's group integrated voltammetry and electrochemical impedance spectroscopy (EIS) with ESI-MS to develop VESI-MS and EIS-ESI-MS, enabling real-time tracking of electrochemical intermediates during CV scanning (Fig. 6a).[74] This approach establishes critical correlations between voltammetry responses and detected species, revealing diffusion-layer dynamics governing electrode reactions. Nevertheless, this EC-MS technique remains constrained to monitoring fleeting intermediates due to inherent species transfer delays from the electrode to the MS inlet. Recently, Chen's group presented a time-resolved *operando* EC-MS platform through integration of a functionalized electrochemical microreactor with nESI-MS for stepwise monitoring of reactive intermediates in electrosynthesis across both direct current (DC) and alternating current (AC) regimes.[28] As illustrated in Fig. 6b, two Pt wire electrodes were inserted into a glass capillary, in which the Pt wire WE at the tip ensures the rapid transfer of short-lived intermediates into gas-phase ionization for MS detection. By employing adjustable DC or AC power (μA to mA), this system effectively simulates practical electrosynthetic conditions and significantly accelerates reactions. Furthermore, building on a previously established FE-ESI-MS platform, Wei's group successfully monitored and characterized transient intermediates in real time during the electrochemical processes, providing molecular evidence for the reaction pathways between indole radical cations and various partners in the dearomatizing esterification reaction (Fig. 6c).[75] Such detailed insights into the formation of these dynamic active intermediates are vital for pioneering new reactivity and promoting efficient, lasting electrochemical processes. In addition, by constructing an electrochemical flow cell within a pneumatic spray device and coupling it with atmospheric pressure chemical ionization (APCI), Cui *et al.* proposed a step scanning voltage EC-MS (SSV-EC-MS) and achieved the direct capture and APCI-MS analysis of freshly formed intermediates, in which the APCI

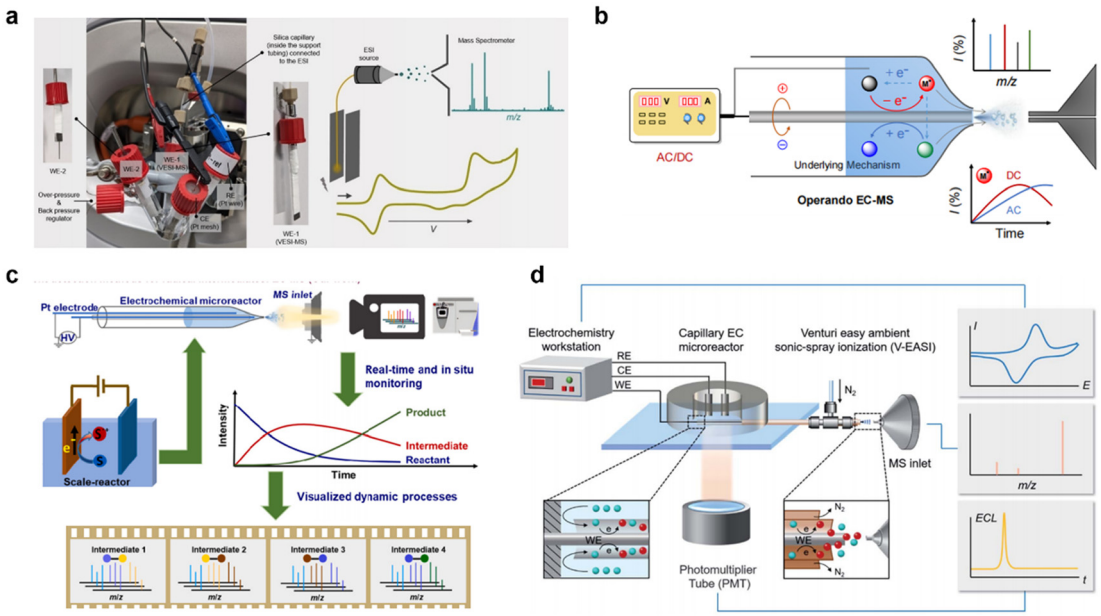

Fig. 6 (a) Schematic illustration of the EC-MS setup integrated voltammetry into ESI-MS (VESI-MS). Reprinted with permission from ref. 74. Copyright (2024) Wiley-VCH. (b) Schematic of the time-resolved *operando* EC-MS platform. Reprinted with permission from ref. 28. Copyright (2023) Wiley-VCH. (c) Working process of the FE-ESI-MS setup for the real-time tracking of the intermediate dynamics. Reprinted with permission from ref. 75. Copyright (2024) The Royal Society of Chemistry. (d) Schematic of the RT-Triplex platform for electricity-luminescence-mass synchronization. Reprinted with permission from ref. 77. Copyright (2022) The Royal Society of Chemistry.

boosted sensitivity for low-polarity species and decoupled ionization from EC control.[76]

Correlating multiple parameters, specifically mass spectrometric and electrochemical signals, in real time during electrochemical processes allows for the determination of each electron transfer event at the molecular level, leading to a deeper comprehension of electrochemical reaction mechanisms and aiding the dissection of complex reaction networks. Aiming to correlate the signals of short-lived intermediates with the applied potentials, our group designed and constructed an integrated mass spectrometric platform (RT-Triplex) for real-time acquisition and synchronization of electrical, luminescence, and mass spectrometric signals during dynamic EC/ECL processes.[77] As shown in Fig. 6d, by integrating a homemade capillary electrochemical microreactor, a photomultiplier tube (PMT) and a Venturi easy ambient sonic-spray ionization mass spectrometer (V-EASI-MS), this RT-Triplex not only identifies the electrochemical short-lived intermediates with sub-millisecond half-lives but also tracks and distinguishes multi-step electrochemical redox processes involving multi-electron transfers at high potentials and with temporal resolution.

Time-of-flight secondary ion mass spectrometry (ToF-SIMS) can perform real-time sample detection through the analysis of secondary ions liberated from a sample surface by primary ion bombardment under a high vacuum.[78,79] Nevertheless, the necessity for a high-vacuum environment restricts its capability for *in situ*, real-time monitoring of electrochemical reactions. To address this limitation, Zhu and Yu's group pioneered an *in situ* liquid ToF-SIMS technique by integrating ToF-SIMS with a vacuum-compatible microfluidic electrochemical device for *in situ* analysis of the solid–liquid interfaces.[80] As shown in Fig. 7a, this EC-MS platform utilizes a silicon nitride (SiN) membrane to isolate the electrolyte within the electrochemical cell from the vacuum environment. A primary ion beam subsequently etches a 1–2 μm diameter

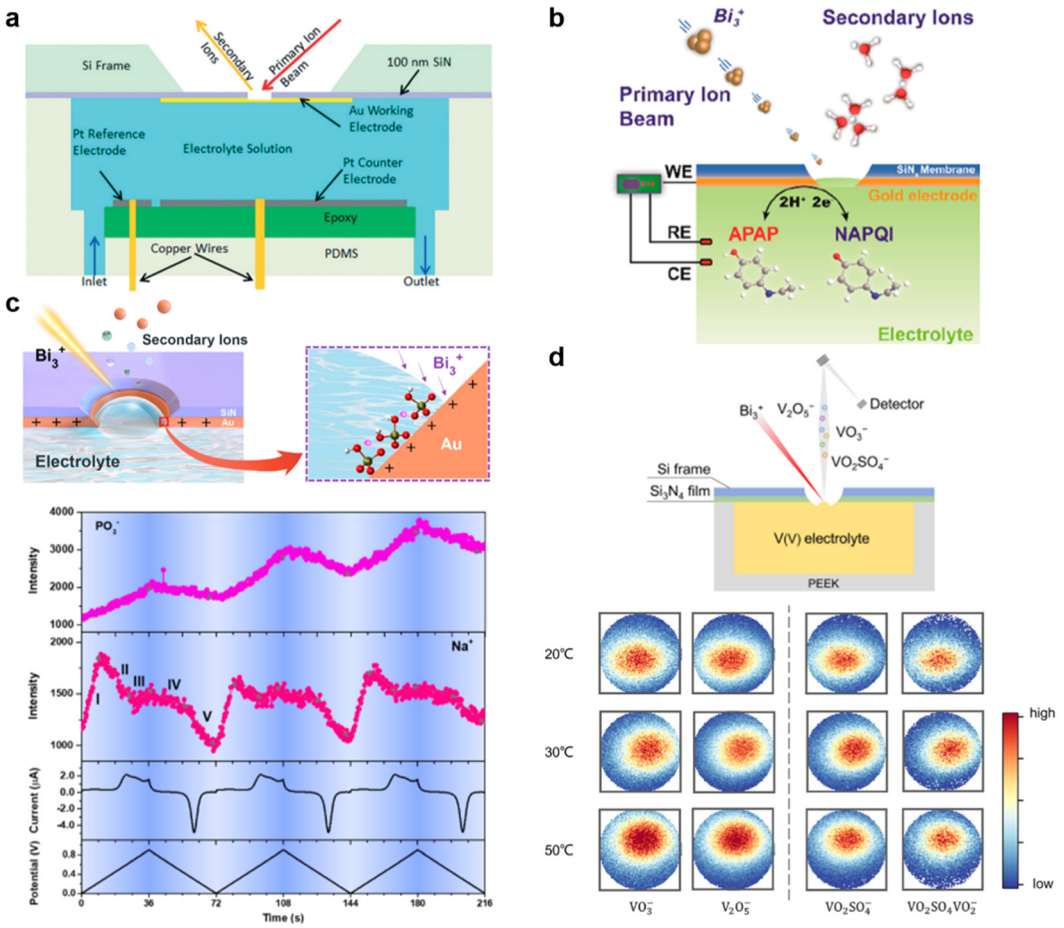

Fig. 7 (a) Schematic illustration of the side view of *in situ* liquid ToF-SIMS. Reprinted with permission from ref. 81. Copyright (2017) American Chemical Society. (b) Schematic of *in situ* liquid ToF-SIMS coupled with an electrochemical workstation for probing EEIs during an electrochemical reaction of APAP. Reprinted with permission from ref. 82. Copyright (2019) American Chemical Society. (c) Schematic of *in situ* liquid ToF-SIMS measurement through the microaperture drilled by the primary Bi_3^+ ions and the potential-resolved signal trends during the potential scan on the gold electrode surface. Reprinted with permission from ref. 84. Copyright (2021) American Chemical Society. (d) *In situ* liquid ToF-SIMS chemical mapping of key ionic species at 20 °C, 30 °C, and 50 °C, showing the increased formation of VO_3^- and $V_2O_5^-$ at elevated temperatures while anion-coordinated species $VO_2SO_4^-$ and $VO_2SO_4VO_2^-$ remain relatively stable. Reprinted with permission from ref. 85. Copyright (2025) Wiley-VCH.

micro-aperture through the SiN membrane, enabling *in situ* analysis of the confined liquid surface within the microporous region. Compared to EC-MS methods based on ESI-MS and AIMS, *in situ* liquid ToF-SIMS provides exceptional surface sensitivity and nanoscale information depth. This technique allows simultaneous *in situ* ionization of both solid surfaces and liquid phases at EEIs, thereby enabling real-time characterization of the electric double layer at the nanoscale.[81] Zhu's group adopted the electrochemical reactions of acetaminophen (APAP) as a mimetic cytochrome P450 catalytic metabolism and employed ToF-SIMS to directly track the release and recombination of hydrated protons at the EEIs during the electrochemical reaction of APAP (Fig. 7b).[82] Zhang *et al.* utilized *in situ* liquid ToF-SIMS to investigate the electrocatalytic oxidation of ethanol on a gold electrode in an alcohol fuel cell system. By correlating the real-time signals obtained from the surface of the gold electrode at different potentials with the oxidation products, the surface adsorbed hydroxide intermediates characterized by $Au_xOH_y^-$ ions were molecularly determined to be the active surface sites on gold governing the electrocatalytic process.[83] Building on prior research, Zhang *et al.* investigated the formation and evolution of the EEIs between a gold electrode and phosphate buffer solution and found that sodium cations form ion pairs with phosphate anions (PO_3^-) on the positively charged gold electrode surface, resulting in a dense adsorption phase to retard electrochemical reactions (Fig. 7c).[84] Recently, Mu *et al.* revealed the solvation structure and chemistry transformation mechanism of V(v) electrolytes in vanadium flow batteries (VFBs) through atomic-level simulations and *in situ* liquid ToF-SIMS characterization studies (Fig. 7d). Through *in situ* liquid ToF-SIMS monitoring of the thermal behavior of V(v) solvated species in electrolytes, they have clarified the transformation from $[VO_2(H_2O)_3]^+$ to $VO(OH)_3$, identifying the second deprotonation as the rate-determining step in VFBs.[85]

3. Applications of EC-MS methods in mechanistic investigation of electrochemical reactions

3.1 Organic electrosynthesis

Organic electrosynthesis directly employs electrons to drive redox reactions, providing a robust and environmentally benign strategy for the selective synthesis of target molecules.[86–88] In recent years, EC-MS methods, characterized by high sensitivity and specificity, have been harnessed for the detection of fleeting intermediates and the screening of potential substrates in organic electrosynthesis, serving as a powerful tool for investigating reaction mechanisms and uncovering hidden reaction pathways.[89] As a crucial aspect of studying electrochemical reaction mechanisms, determining the initial step offers fundamental insights into how these reactions commence. However, this initial step frequently involves a one-electron transfer, generating unstable radical cations or anions, which consequently poses significant experimental challenges. For this purpose, Zare and Chen's group developed a novel EC-MS platform featuring a "waterwheel" (WE) integrated with DESI-MS and achieved the first mass spectrometric snapshots of DMA radical cations, a key intermediate produced during the one-electron oxidation of DMA.[20] Regarding the electrochemical oxidation of ANI, Jiang's group utilized an EC-DSI-MS setup to rapidly capture the ANI radical cations formed upon the one-electron oxidation of ANI.[63] In addition to the detection of radical cations or anions generated in the initial step of electrochemical reactions, the direct observation of the electrochemically generated nitrenium ions from the electrooxidation of 4,4-dimethyoxydiphenylamine (DMDPA) and di-*p*-tolylamine (DPTA) was achieved at the molecular level by using EC-DESI-MS.[90]

Understanding the reaction mechanisms of organic electrosynthesis relies on identifying key intermediates along the reaction pathway, as these often dictate the reaction outcomes. Therefore, direct observation of these intermediates provides invaluable insights into the underlying electrochemical processes.[58] Chen's group reported the detection of short-lived carbazole radical cations from the electrooxidation of carbazole using EC-DESI-MS. Following the successful observation of these key intermediates, they have clarified the carbazole dimerization mechanism, demonstrating that it proceeds *via* the reaction of one radical cation with one neutral molecule, rather than the previously proposed coupling of two radical cations (Fig. 8a).[91] Utilizing a home-built EC-MS platform, the reactivity between *N*-cyclopropylaniline radical cation toward alkenes was explored by their group (Fig. 8b). Based on the molecular information obtained from this reaction, a novel redox-neutral reaction pathway involving intermolecular [3 + 2] annulation between *N*-cyclopropylanilines and alkenes was uncovered, which directly affords an aniline-substituted 5-membered carbocycle through direct electrolysis, with yields reaching up to 81%.[92] Additionally, the degradation pathway of ciprofloxacin removal *via* the electro-Fenton-like process was verified by mass spectrometric detection of six characteristic intermediates.[93] As shown in Fig. 8c, Hu *et al.* employed an EC-MS based hybrid BPE and nESI-MS to reveal a previously hidden nitrenium ion involved in the reaction pathway in the C–H/N–H cross-coupling reaction between DMA and phenothiazine (PTA) by detecting the key intermediate nitrenium ion.[94] Based on FE-ESI-MS, Wei's group identified several nitrene intermediates, thereby revealing a hidden reaction pathway in which nitrene formation plays a crucial role in the electroreductive coupling process.[64] Recently, through the capture of key intermediates, Wei's group collaborated with Lei's group to provide the molecular-level evidence for the reaction between indole radical cations and both radical precursors and nucleophilic reagents, guiding the development of an electrochemical dearomatizing esterification of indole and synthesis of a diverse array of 3,3-disubstituted oxindoles with notable regioselectivities (Fig. 8d).[75] In addition, the molecular evidence for the formation of α-amino radical cations and iminium cations in the electrochemical oxidative α-C(sp^3)–H

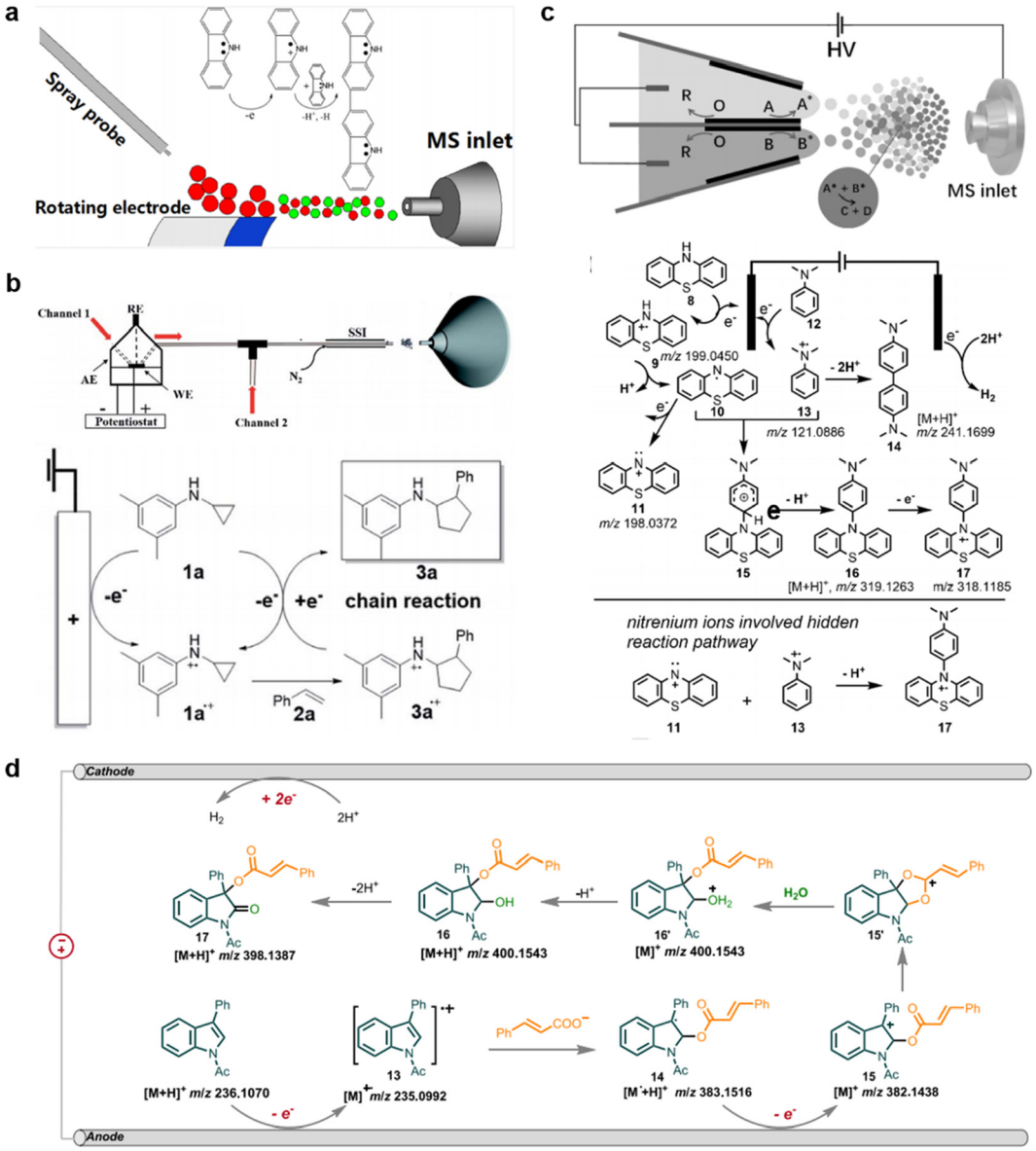

Fig. 8 (a) Proposed oxidation and dimerization pathway of CBZ verified by the EC-MS setup with the rotating waterwheel WE. Reprinted with permission from ref. 91. Copyright (2020) American Chemical Society. (b) Schematic of an EC-MS platform for the mechanistic study of the [3 + 2] annulation reaction of *N*-cyclopropylanilines and styrene. Reprinted with permission from ref. 92. Copyright (2020) The Royal Society of Chemistry. (c) Schematic of an on-the-fly microdroplet based microreactor for mass spectrometric probing of the flash chemistry of electrogenerated intermediates and the proposed mechanism for cross-coupling between DMA and PTA. Reprinted with permission from ref. 94. Copyright (2021) Wiley-VCH. (d) Proposed pathway of the electrochemical oxidative dearomatizating esterification reaction of 3-phenyl *N*-acetyl indole and cinnamic acid verified by FE-ESI-MS. Reprinted with permission from ref. 75. Copyright (2024) Cell.

functionalization of tertiary amines was provided by utilizing BPE-nESI-MS.[95] In addition to the interfacial electrochemical reactions at heterogeneous EEIs, organic electrosynthesis reactions also involve homogeneous processes in the electrolyte. To address this complexity, our group developed a decoupled electrochemical flow microreactor hyphenated mass spectrometry platform (DEC-FMR-MS), which enables segmented mechanistic investigation of electrode and homogeneous processes by tracking the fate of key intermediates. Leveraging this approach, we discovered two hidden quasi-electrocatalytic pathways mediated by nitrenium ions and *N*,*N*,*N*′,*N*′-tetramethylbenzidine radical cations ($TMB^{\bullet+}$) in electrooxidative C–H/N–H cross-coupling. Moreover, we elucidated homogeneous reaction routes initiated by alkene radical cations and nitrenes during electrochemical aziridination at the molecular level.[96]

Regarding the electrosynthesis mediated by molecular catalysts, Wan *et al.* utilized an EC-nESI-MS method (Fig. 9a) to investigate the mechanism of the TEMPO-mediated dehydrogenation of THQ by capturing several key intermediates such as $TEMPO^{+}$, TEMPOH, and 1,2-dihydroquinoline.[51] Building

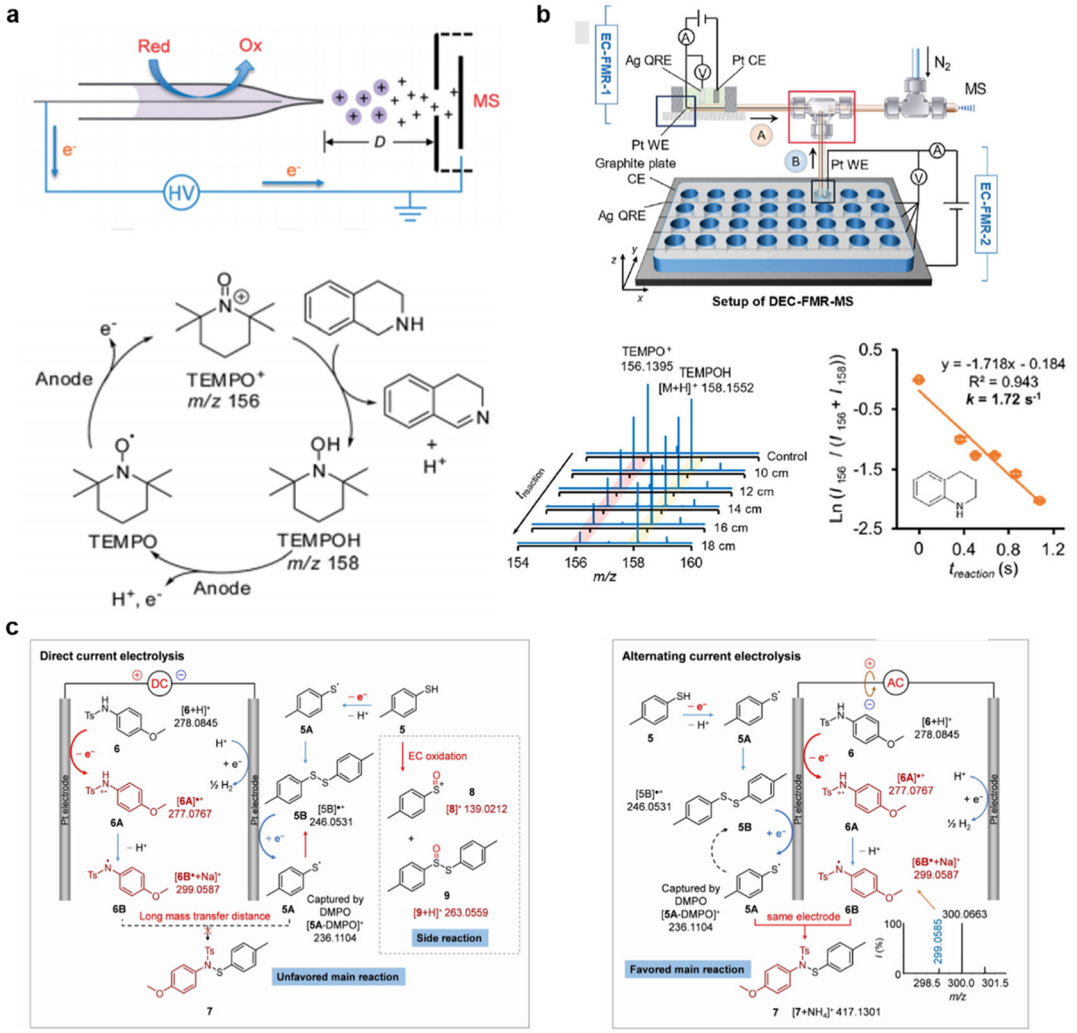

Fig. 9 (a) Schematic illustration of the real-time electrochemical reaction platform and the proposed mechanism of TEMPO-mediated oxidation of THQ. Reprinted with permission from ref. 51. Copyright (2018) The Royal Society of Chemistry. (b) Schematic of a decoupled electrochemical flow microreactor hyphenated mass spectrometry platform (DEC-FMR-MS), and positive-ion-mode mass spectra and the plot of ln ($I_{156}/(I_{156} + I_{158})$) against reaction time for the reaction between electrochemically generated $TEMPO^+$ and THQ operated at different lengths of the mixing capillary. Reprinted with permission from ref. 96. Copyright (2025) Nature. (c) Proposed mechanism of the N–S bond formation reaction under DC and AC electrolysis. Reprinted with permission from ref. 28. Copyright (2023) Wiley-VCH.

on this, Li *et al.*, using an electrochemical extraction electrospray ionization mass spectrometry (EC-EESI-MS) setup, found that $TEMPO^+$ reacts with THQ *via* electron transfer to produce $THQ^{\bullet+}$ and TEMPOH. Subsequently, $THQ^{\bullet+}$ converts to dihydroquinoline in solution, while TEMPOH is reoxidized at the electrode to regenerate $TEMPO^+$, which leads to the continuous dehydrogenation of dihydroquinoline to quinoline (Fig. 9b).[97] Recently, our group employed DEC-FMR-MS to measure the kinetics of the TEMPOH-mediated dehydrogenation reaction of N-heterocycles. The kinetic measurements revealed that THQ cores substituted with electron-donating groups on the benzene ring exhibited faster kinetics than those bearing electron-withdrawing moieties.[96] In recent years, the unique ability of alternating current (AC) electrolysis to facilitate both oxidation and reduction processes on the same electrode surface, unlike direct current (DC) electrolysis, has drawn considerable attention in the field of electroorganic synthesis. Wan *et al.* proposed a time-resolved EC-MS platform to study the reaction mechanism of AC electrosynthesis under *operando* electrosynthetic conditions and verified the unique reactivities of AC electrosynthesis. Direct verification of effective cross-coupling between transient sulfur- and nitrogen-centered radicals, generated *via* AC electrolysis, was achieved through rapid capture of neutral radicals, while time-resolved intermediate mapping revealed AC electrolysis kinetic control over N-radicals to suppress homocoupling pathways in multistep electrosynthesis (Fig. 9c).[28]

3.2 Electrocatalysis

Given the pressing demand for advancements in clean energy technologies, electrocatalysis employs catalysts to improve reaction kinetics and boost selectivity by lowering electro-

chemical reaction energy barriers, contributing sustainable solutions to the discovery and utilization of alternative energy sources.[98,99] Real-time monitoring of electrode interface processes and rapid capture of critical intermediates yield mechanistic insights that direct catalyst design and selectivity optimization. Recently, EC-MS technology has shown significant promise in dissecting complex electrocatalytic reaction networks. The significant CO_2 emissions from chemical manufacturing have spurred the pursuit of sustainable electrocatalytic CO_2 conversion technologies.[100] DEMS has emerged as a powerful tool for mechanistic investigations of the electrocatalytic CO_2RR, owing to its ability to provide real-time, high-sensitivity monitoring of both gaseous and volatile liquid products under *operando* conditions. Guo *et al.* employed online DEMS to track ion signals of H_2, CO, and formate during the CO_2RR on Bi@C-700-4 catalysts, elucidating the potential-dependent onset of formate production and its correlation with high catalytic selectivity.[101] Utilizing DEMS to track product evolution during pulsed electrolysis of CO_2 on silver and copper electrodes, Ye *et al.* discovered that anodic pulses play a crucial role, which trigger surface reconstruction and modify the interfacial environment, consequently boosting local CO_2 levels and improving CO_2RR selectivity.[102] In addition, the combination of an isotope labeling strategy with DEMS offers a powerful means for tracking carbon transformation pathways, identifying the origins of intermediates and products, and elucidating complex reaction mechanisms. For instance, DEMS was employed to measure the ion signals of $^{12}CO_2$, $^{13}CO_2$, ^{12}CO, and ^{13}CO during the electrocatalytic CO_2RR, therefore confirming the existence of two CO_2 transfer pathways. As shown in Fig. 10a, by introducing $^{12}CO_2$ and $H^{13}CO_3^-$ into the electrolytic cell under both open-circuit and applied-potential conditions, the critical transport role of HCO_3^- in facilitating CO_2 formation *via* rapid buffer reactions was revealed.[103]

To tackle nitrate pollution and reduce the energy burden of ammonia production, the electrocatalytic nitrate reduction reaction (NO_3RR) is emerging as a viable and increasingly researched technology.[104] In this context, EC-MS has proved indispensable for elucidating reaction dynamics through real-time monitoring of nitrogen species, thereby guiding catalyst optimization strategies. Furthermore, recent work underscores the versatility of DEMS in dissecting NO_3RR mechanisms across a wide array of catalysts. Wang *et al.* applied online DEMS to track key nitrogen intermediates, such as NO_2, NO, NH_2OH, and NH_3, during the electrocatalytic NO_3RR on Cu/Cu_2O nanowires, revealing a stepwise hydrogenation pathway where *NO-to-*NOH conversion governs selectivity (Fig. 10b).[105] Han *et al.* combined DEMS with ^{15}N isotope labeling to trace ammonia formation during the NO_3RR on RuCo alloys. Through real-time MS monitoring under potential cycling, dynamic alterations in nitrogen species were observed, validating a complex three-step relay mechanism encompassing spontaneous redox, electrochemical reduction, and electrocatalytic conversion.[106] Zhang *et al.* used DEMS to study the NO_3RR on Fe/Cu diatomic catalysts, identifying NO as the main intermediate and NH_3 as the predominant product, supporting a reaction network with both dissociative and associat-

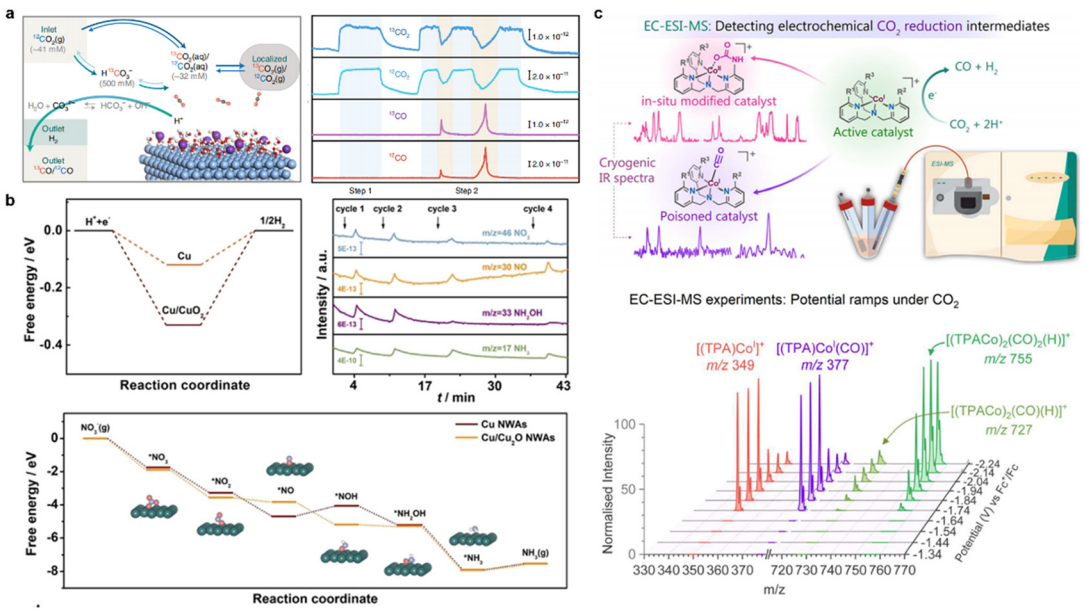

Fig. 10 (a) Proposed pathway of the carbon cycle and DEMS signals from the produced gaseous CO and residue CO_2 during the electrocatalytic CO_2RR. Reprinted with permission from ref. 103. Copyright (2022) Springer Nature. (b) The reaction energies of H_2 formation, DEMS measurements, and the free-energy diagram for the electrocatalytic NO_3RR to ammonia on Cu/Cu_2O nanowires. Reprinted with permission from ref. 105. Copyright (2020) Wiley-VCH. (c) Schematic illustration of the EC-ESI-MS setup and the obtained mass spectra in the CO_2RR catalyzed by Co(II)-TPA. Reprinted with permission from ref. 110. Copyright (2024) American Chemical Society.

ive pathways.[107] Furthermore, with recent advances *in operando* DEMS, the mechanistic studies have been extended to complex C–N coupling processes, revealing the dynamic interactions between nitrogen-containing intermediates and carbon-based reactants that affect product selectivity. In pulsed co-electrolysis for urea synthesis, DEMS revealed alternating CO and NH_2 signal intensities at carbon nanotube electrodes coated with an iron tetraphenylporphyrin (FeTPP) catalyst, confirming potential-dependent accumulation of *CO and $*NH_2$ intermediates crucial for C–N bond formation.[108] In addition to the CO_2RR and the NO_3RR, Lucky *et al.* utilized EC-MS to investigate the potential-dependent distribution of surface compounds in the electrocatalytic oxidation of methane on Pt electrodes. Through direct measurement of adsorbate oxidation products, they revealed that methane adsorption exhibits strong potential dependence, peaking at 0.3 V *vs.* RHE. Furthermore, they identified *CO as the dominant surface intermediate, regardless of the methane adsorption potential.[109]

Beyond the crucial capability of EC-MS for online detection of gaseous and volatile products, the rapid capture of liquid-phase metastable intermediates offers equally vital, direct evidence essential for unraveling the intricate mechanisms underlying electrocatalytic reactions. Bairagi *et al.* developed a general EC-MS platform to identify key intermediates in the CO_2RR catalyzed by a series of cobalt complexes featuring tris (2-pyridylmethyl)amine (TPA)-ligands with amino group modifications in the secondary coordination sphere (Fig. 10c). By combining the EC-MS experiments with density functional theory (DFT) calculations, they revealed that the by-product Co (I)-carbonyl species acts as a catalyst poison during CO_2-to-CO conversion. Furthermore, protonation of Co(I) complexes also initiates the HER, which is subsequently amplified by *in situ* conversion of secondary sphere amino groups to carbamate, thereby accelerating H_2 evolution.[110] In the context of other electrocatalytic reactions, such as the electrochemical oxygen reduction reaction (ORR), Shao's group utilized EC-MS to investigate the oxygen reduction reaction (ORR) catalyzed by ferrocene (Fc) and cobalt tetraphenylporphyrin (CoTPP) at the liquid/liquid interface. The key intermediates, (Co(II)-O_2)TPP and (Co(III)-OH)TPP, were identified during this reaction process, elucidating the four-electron pathway of ORR (Fig. 11a).[69] Recently, this research group successfully detected crucial iron–oxygen intermediates using an *in situ* EC-MS setup, thus providing detailed experimental evidence for the catalytic cycle of the ORR catalyzed by $[Fe(III)TPP]^+$ and indicating a $4e^-/4H^+$ mechanism of this reaction.[111] By integrating current responses obtained from CV and EIS with dynamic intermediate profiles collected *via* ESI-MS, Surendran *et al.* detected various reaction intermediates and revealed degradation pathways in the ORR catalyzed by an iron tetraphenyl porphyrin (FeTPP) complex under different kinetic regimes (Fig. 11b).[112] Furthermore, Shao's group directly observed key short-lived intermediates during water oxidation catalyzed by a cobalt-tetraamido macrocyclic ligand complex (CoTAML) using an EC-MS method.[113] This important observation further confirmed the possibility of a water nucleophilic attack mechanism for the single-site water oxidation catalysis at the molecular level (Fig. 11c).[113] Recently, Cheng *et al.* surprisingly discovered that the reactive transition metal cations, such as Pd (II) species, could be generated due to the anodic corrosion of the Pd electrode in the ion emitter of nESI, which further cata-

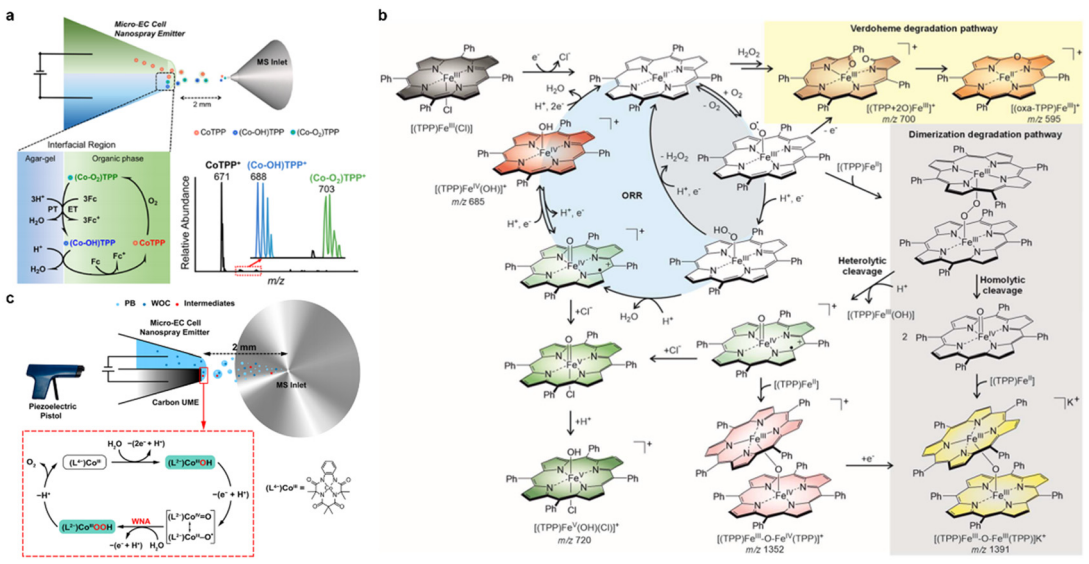

Fig. 11 (a) Schematic illustration of the EC-MS setup with the gel hybrid ultramicroelectrode functioning as the micro-EC cell/nanospray emitter and the proposed mechanism of the ORR consisting of H^+ in agar-gel and Fc in the organic phase catalyzed by CoTPP. Reprinted with permission from ref. 69. Copyright (2019) American Chemical Society. (b) The electrocatalytic ORR mechanism catalyzed by Fe(II)(TPP). Reprinted with permission from ref. 112. Copyright (2024) American Chemical Society. (c) Schematic illustration of the *in situ* EC-MS setup and the proposed mechanism of water oxidation catalyzed by Co(III)-TAML. Reprinted with permission from ref. 113. Copyright (2022) American Chemical Society.

lyzed the cascade Suzuki coupling/electrochemical C–H arylation at room temperature. Plausible catalytic routes of cascade Pd-catalyzed Suzuki coupling/electrochemical C–H arylation were proposed on the basis of observed multiple key Pd intermediates. More importantly, this EC-MS platform showcases the capability of integrating an electrochemical microreactor with MS, which greatly aids mechanistic studies by capturing various intermediates.[18]

3.3 Lithium-ion batteries

Lithium-ion batteries (LIBs) power a wide array of applications from portable electronic devices and electric vehicles to grid-scale renewable energy storage systems, owing to their high energy density, long cycle life, low self-discharge rate, and robust performance across diverse environmental conditions.[114] However, significant debate persists regarding the lithium-ion solvation process and the formation mechanism and the composition of the solid electrolyte interphase (SEI).[115,116] In recent years, the development of EC-MS has made it possible to monitor the chemical composition of SEI, enabling a world of possibilities for deeply investigating the complex physical and chemical processes occurring at EEI in LIBs. Among them, *in situ* ToF-SIMS with its unique capability for spectrally and depth-resolved data offers a potent means to elucidate SEI composition, investigate electrolyte degradation pathways, and map reaction zones across LIB interfaces. In response to the volatile electrolyte environment of LIBs, Zhu *et al.* firstly designed a specific liquid cell device to integrate ToF-SIMS, allowing for the investigation of lithium plating and stripping dynamics on a copper electrode. Through in-depth profiling of representative secondary ions from both positive and negative electrodes, they discovered that Li metal deposition on copper induces solvent condensation. This process establishes a lean electrolyte layer near the electrode which is depleted of salt anions and Li^+, thereby contributing to the overpotential of LIBs. Their finding provides unique insights into molecular-level dynamics of initial SEI formation.[117]

Solvation plays a key role in determining the transport rates of lithium ions, the stability of the electrolyte, and the dynamics of SEI formation. *In situ* liquid ToF-SIMS requires no liquid pretreatment procedures, such as desalination, enabling direct probing of solvation structures in electrolytes. Leveraging this capability, Wang and Zhu's group utilized *in situ* ToF-SIMS to analyse lithium bis(fluorosulfonyl)imide/1,2-dimethoxyethane (LiFSI/DME) and lithium hexafluorophosphate/ethylene carbonate-dimethyl carbonate ($LiPF_6$/EC-DMC) systems in LIBs. Their investigation has shown that Li^+ ions are predominantly solvated by EC molecules within the $LiPF_6$/EC-DMC system, and a subtle attractive force is detected between EC and PF_6^- ions as well.[118] Zhang *et al.* investigated the chemical evolution during high-temperature calendar aging at the anode/electrolyte interfaces in $LiPF_6$ and LiFSI electrolyte systems by using *in situ* liquid ToF-SIMS. Representative *in situ* liquid ToF-SIMS spectra in the positive and negative ion modes of the $LiPF_6$-based and the LiFSI-based electrolyte were recorded before and after high-temperature calendar aging for 6 d, highlighting the signals of ions related to hydrolysis and showing their intensity evolution (Fig. 12). Drawing on these observations, they identified that at high temperatures, trace H_2O preferentially attacks anion aggregates in $LiPF_6$, triggering its hydrolysis. The resulting inorganic compounds aid in constructing an inorganic-rich SEI, enhancing anode stability. Conversely, LiFSI-based electrolytes are hydrolysis-resistant, leading to the preferential formation of an organic-rich SEI.[119]

During charge and discharge cycles, the complex chain reactions linked to the decomposition of electrodes and electrolyte materials can trigger gas evolution inside the LIBs, which not only undermines their energy storage capacity but also poses significant safety risks.[120] Based on real-time detection of various gaseous reaction products, DEMS allows for detailed investigation of SEI formation, irreversible capacity loss, degradation pathways, overpotential evolution, interfacial stability, and gas evolution processes.[38,121] By combining DEMS and MS titration, McShane *et al.* characterized graphite SEI formation under varying $LiPF_6$ concentrations by detecting and quantifying gas evolution (H_2, C_2H_4, and CO_2). The results revealed that increasing the $LiPF_6$ concentration leads to a thicker inner SEI rich in LiF and a thinner outer SEI rich in alkyl carbonates, ultimately resulting in a thinner overall SEI,

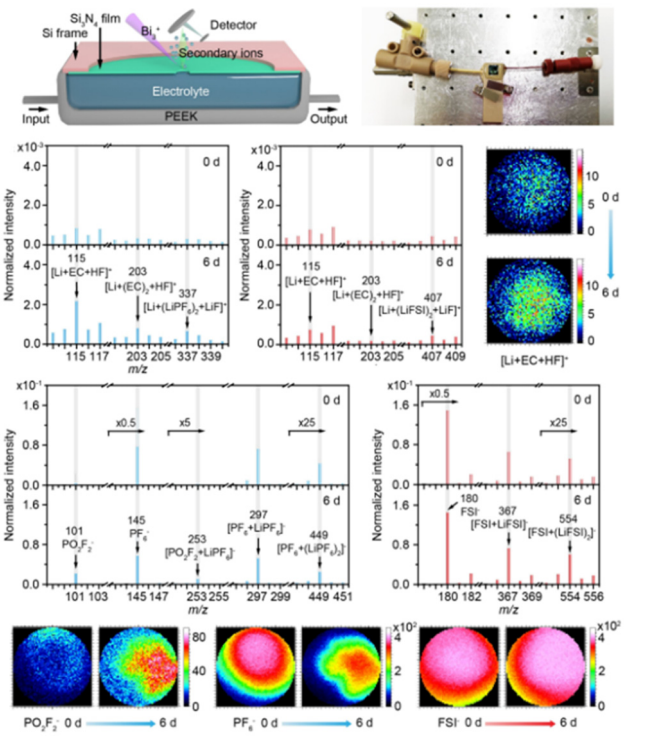

Fig. 12 Schematic illustration and photograph of the assembly of the ultrahigh-vacuum compatible microfluidic device, and representative *in situ* liquid ToF-SIMS spectra in the positive and negative ion modes of the $LiPF_6$-and LiFSI-based electrolytes before and after high-temperature calendar aging for 6 d (144 h), highlighting the signals of ions related to hydrolysis and showing their intensity evolution. Reprinted with permission from ref. 119. Copyright (2025) Wiley-VCH.

while the deposited LiEDC is transformed into LiEMC by HF and further converted into noncarbonate species through a host of other reactions (Fig. 13a).[122] Nakanishi's group utilized the Br^-/Br^{3-} redox couple as a model mediator to investigate its mitigating effects on Li_2O_2 formation and decomposition in Li–O_2 batteries. Through a combination of nanoscale secondary ion mass spectrometry (Nano-SIMS) isotopic 3D imaging and DEMS analyses, they have observed that the oxidative decomposition of Li_2O_2 is highly dependent on the cell voltage and discovered that accelerating the redox mediator's reaction rate at the Li_2O_2/electrolyte interface is crucial for enhancing battery cycle life.[123] Furthermore, the high solubility of long-chain polysulfides in Li–S batteries allows them to permeate through the separator membrane during charge–discharge cycles, causing self-discharge and lithium dendrite growth, which in turn lead to capacity degradation and safety concerns. Shao's group investigated the distribution of polysulfides at different potentials using an *in situ* EC-MS platform and subsequently selected cobalt phthalocyanine (CoPc) as a model electrocatalyst to study the catalytic conversion of polysulfides. By capturing a series of CoPc-lithium polysulfide complex intermediates and mapping the distribution of various polysulfides at different potentials, they demonstrated the selective catalytic activity of CoPc toward long-chain polysulfides (Fig. 13b).[124]

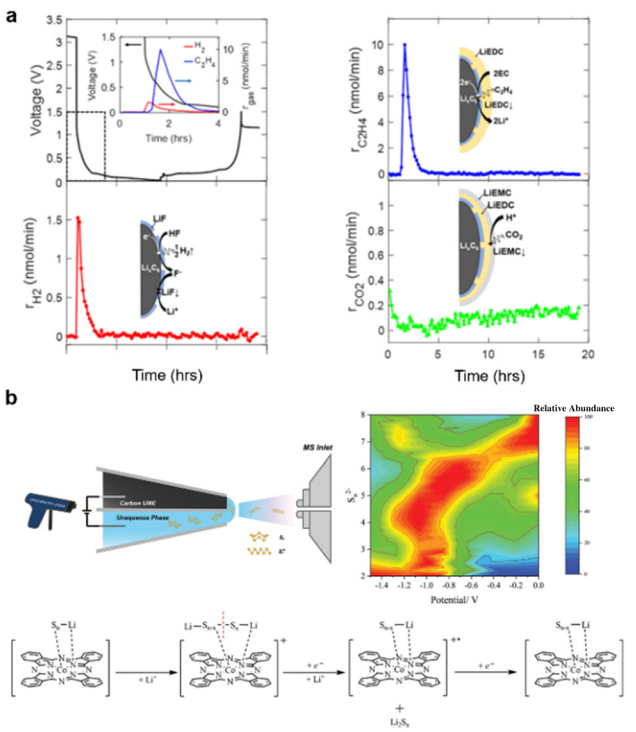

Fig. 13 (a) The DEMS measurements of generated gases in the first formation cycle of a Li-graphite cell. Insets show the proposed mechanism of LiF deposition, LiEDC deposition, and the LiEMC chemical formation mechanism. Reprinted with permission from ref. 122. Copyright (2022) American Chemical Society. (b) Schematic of the EC-MS setup, relative abundance distribution of various polysulfides at various potentials estimated from the EC-MS data, and the proposed pathway of the electrolytic polysulfide conversion process with CoPc as an electrocatalyst. Reprinted with permission from ref. 124. Copyright (2021) Wiley-VCH.

3.4 ECL

ECL is light emission from excited luminophores formed by redox reactions at EEI. Understanding the ECL mechanisms is vital for improving luminescence efficiency, developing novel luminophore systems, and building selective, stable sensors.[125,126] Although conventional electrochemical and spectroscopic methods offer insights into electron transfer and energy level transition during ECL processes, they fall short in revealing the detailed chemical transformation at the molecular level.[127,128] Recently, EC-MS, capable of rapidly capturing transient intermediates at the electrode surface, has provided significant advantages for mapping reaction pathways in complex electrochemical systems, thereby broadening its utility for advancing ECL mechanistic studies. The $Ru(bpy)_3^{2+}$/TPrA system stands out as one of the most widely employed ECL systems, with its mechanism having been thoroughly investigated *via* the synchronous measurement of luminescence and electrochemical signals during CV and step scanning.[129,130] Despite this progress, obtaining a comprehensive molecular-level understanding of the ECL process continues to pose a significant challenge. Utilizing an EC-MS setup with a hybrid ultramicroelectrode, Shao's group identified two ECL pathways in the $Ru(bpy)_3^{2+}$/TPrA system (Fig. 14a). Applying 0.8 V to the electrode allowed the detection of key intermediates $[Pr_2N{=}CHCH_2CH_3]^+$, $[NHPr_2]^+$, and $Ru(bpy)_3^+$, corroborating the ECL "revisited route" at the molecular level. At a higher potential (1.3 V), the intermediate $Ru(bpy)_3^{3+}$ was observed, which is then reduced to luminescent $Ru(bpy)_3^{2+}$* *via* co-reactant involvement.[68] This group subsequently employed EC-MS to study the ECL behavior of the novel luminophore $Ir(ppy)_3^+$ by comparing the relative intensity in the presence and absence of TPrA across different potentials (Fig. 14b).[131] Additionally, Hu *et al.* firstly captured the co-reactant TPrA radical cations with a lifetime of approximately 200 μs using a BUME-nESI-MS platform, which are considered to play an essential role in TPrA-mediated ECL.[70] To overcome the limitation of MS in directly detecting transient neutral radicals, Liu *et al.* developed electrochemistry-neutral reionization-mass spectrometry (EC-NR-MS) by connecting an EC flow cell and an easy ambient sonic-spray ionization (EASI) source (Fig. 14c).[132] This setup allowed for the secondary ionization and mass spectrometric analysis of key neutral intermediates with strong reducing properties in ECL reactions, such as the TPrA radical ($TPrA^{\bullet}$), the 2-(dibutylamino) ethanol radical ($DBAE^{\bullet}$), and the triethanolamine radical ($TEOA^{\bullet}$). Collaborating with Su's group, Jiang's group used this EC-NR-MS platform to explore the reactivity of $Ru(bpy)_3^{2+}$ and five co-reactants. By integrating the ECL signals and mass spectra of neutral radicals and radical cations of five co-reactants, including TPrA, DBAE, TEOA, 2,2′-(butylimino)diethanol (BIDE) and 2,2-bis-(hydroxymethyl)-2,2′,2′-nitrilotriethanol (BIS-TRIS), the reactivities of five tertiary amines consisting of

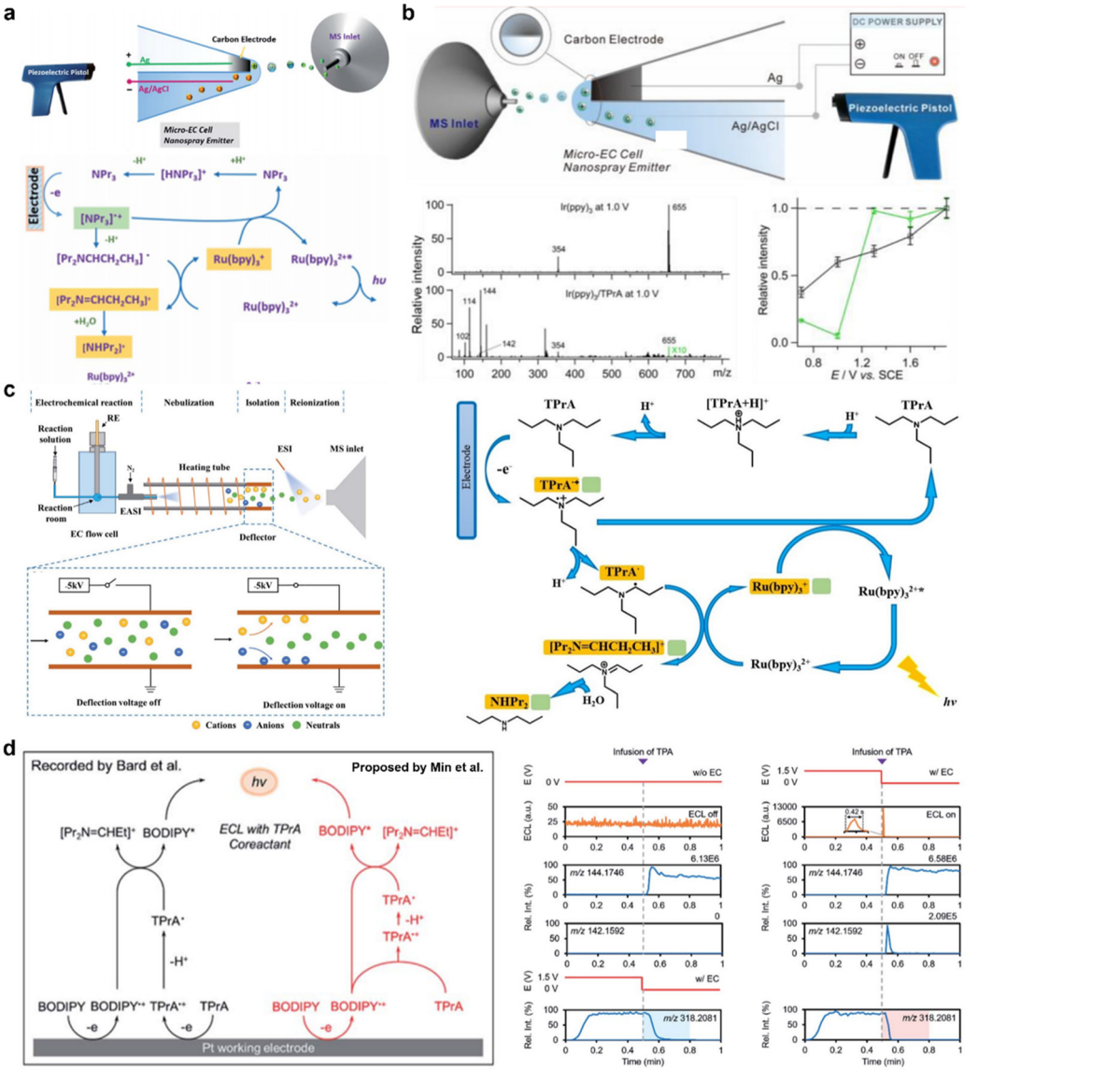

Fig. 14 (a) Schematic illustration of the EC-MS setup containing one micro-carbon electrode and one empty micro-channel, and the "revisited ECL route" of the $Ru(bpy)_3^{2+}$/TPrA system proposed by Bard. Reprinted with permission from ref. 68. Copyright (2016) The Royal Society of Chemistry. (b) Schematic illustration of the EC-MS setup reported by Shao's group, the mass spectra of intermediate $Ir(ppy)_3^{+}$, and the comparison of the relative intensity of $Ir(ppy)_3^{+}$ in the presence and absence of TPrA across different potentials. Reprinted with permission from ref. 131. Copyright (2018) American Chemical Society. (c) Schematic diagram of the basic components of the EC-NR-MS setup, and the working principle of the ion deflector, and the ECL pathway of the $Ru(bpy)_3^{2+}$/TPrA system at a low oxidation potential of 0.8 V. Reprinted with permission from ref. 132. Copyright (2021) The Royal Society of Chemistry. (d) The mechanism for the ECL reaction of the BODIPY/TPrA system proposed by Bard and Min's group, and the applied potential, ECL-time curve and EICs of characteristic ions obtained by modified RT-Triplex. Reprinted with permission from ref. 77. Copyright (2022) The Royal Society of Chemistry.

hydroxyl groups were examined, and the lifetimes of corresponding radical cations were estimated according to the ECL distances in the vertical direction of the electrode surface.[133]

In addition to the $Ru(bpy)_3^{2+}$/TPrA ECL system, Jiang and Su's group verified the $O_2^{\bullet-}$ and $^{\bullet}OH$-mediated cathodic ECL mechanism of an 8-amino-5-chloro-7-phenylpyrido [3,4-*d*]pyridazine-1,4(2*H*,3*H*)-dione (L012)-O_2 ECL system by identifying L012 intermediates. As shown in Fig. 14d, our group employed RT-triplex for the identification of fleeting intermediates and monitoring of ECL dynamic processes in luminol and boron dipyrromethene (BODIPY)/TrPA ECL systems. Due to the synchronization of electrical, luminescence, and mass spectrometric outputs during ECL processes, two ECL pathways of luminol regulated by key intermediates diazaquinone and α-hydroxy hydroperoxide at electrooxidative potentials of 0.3 V and 0.96 V were unraveled, respectively. Moreover, by observing the flash ECL emission and employing a modified RT-Triplex setup, the ECL "catalytic route" of BODIPY involving homogeneous oxidation of TPrA with the BODIPY radical cation is proposed and verified at the molecular level.[77]

4. Summary and outlook

In summary, this review traces the development of EC-MS methodologies for real-time electrochemical reaction monitoring and their deployment across organic electrosynthesis, electrocatalysis, LIBs, and ECL. Traditional approaches, such as DEMS and EC-ESI-MS, serve as foundational techniques for the online analysis of gaseous and liquid reaction products. To achieve rapid detection of transient intermediates, innovative strategies, including minimizing the distance between the EEI and the MS inlet and the integration of ultramicroelectrodes with ESI-MS, have been employed, markedly enhancing temporal resolution. Moreover, EC-MS platforms based on the AIMS technology, capitalizing on their unique capacity for direct molecular interrogation at the EEIs, have demonstrated exceptional efficacy in the capture of short-lived intermediates. The advent of the time- and potential-resolved EC-MS represents a significant advancement, facilitating the dynamic monitoring of fleeting intermediates with superior temporal and potential resolution, thereby elucidating the relationship between the ion signals of electrogenerated species and the applied potentials. Consequently, driven by continuous refinement of its capabilities, EC-MS has emerged as an indispensable analytical tool for probing reaction mechanisms in the fields of organic electrosynthesis, electrocatalysis, LIBs, and ECL.

Although significant efforts have been dedicated to enhancing the temporal and potential resolution of EC-MS in real-time monitoring of electrochemical reactions, the development of *operando* EC-MS techniques, along with their in-depth applications in the electrochemistry field, still lags considerably behind expectations. (1) Current EC-MS achieves excellent temporal and potential resolution but requires cell modifications for MS coupling and ionization, which compromises the fidelity to the real electrochemical reaction conditions. (2) The utilization of high-concentration and non-volatile electrolytes in electrochemical and electrocatalysis reaction systems poses a significant challenge for MS analysis due to severe matrix effects. (3) In light of the growing complexity of electrocatalytic processes, it is crucial to simultaneously characterize electron transfer, chemical changes, and structure evolution in electrochemical systems, as well as to establish the dynamic relationship between molecular and structural variations of EEIs and applied potentials. Gaining such multidimensional insights is essential for deciphering complex electrochemical mechanisms, underscoring the need for integrating complementary analytical techniques.

Addressing the aforementioned drawbacks requires urgent progress in several areas. Firstly, relentless innovation in the coupling of electrochemical cells with MS is critical for achieving real-time monitoring and mechanistic studies of EC reactions under *operando* conditions. The high fidelity of the electrochemical reaction conditions not only bolsters the credibility of mechanism studies but also unlocks potential applications in high-throughput screening of electrochemical reactions, expedited optimization of reaction parameters, and the discovery of novel reaction systems. Subsequently, the development of ionization sources boasting exceptional salt tolerance or sophisticated online desalting methods is a pressing need to broaden the utility of EC-MS in the field of energy electrochemistry. Equally important, the integration of MS with spectroscopic techniques, including FTIR and Raman spectroscopy, into multi-technique platforms constitutes a critical frontier aimed at unraveling electron transfer mechanisms and chemical transformations occurring at EEIs during electrochemical processes. As an emerging and powerful analytical platform, we expect EC-MS technology to assume a more significant role in the mechanistic study of electrochemical reactions.

Conflicts of interest

There are no conflicts to declare.

Data availability

No primary research results, software or code have been included and no new data were generated or analysed as part of this review.

Acknowledgements

The authors would like to acknowledge the National Key Research and Development Program of China (No. 2024YFA1308400), the National Natural Science Foundation of China (No. 22374069), the Fundamental Research Funds for the Central Universities (No. 020514380345), the funding from the State Key Laboratory of Analytical Chemistry for Life Science (No. 5431ZZXM2401), the Guangdong Basic and Applied Basic Research Foundation (No. 2023A1515110224), and the Jiangsu Funding Program for Excellent Postdoctoral Talent (No. 2023ZB442).

References

1 H. Thirsk, *Nature*, 1972, **236**, 290–290.
2 M. C. Leech and K. Lam, *Nat. Rev. Chem.*, 2022, **6**, 275–286.
3 S. Ren, D. Joulié, D. Salvatore, K. Torbensen, M. Wang, M. Robert and C. P. Berlinguette, *Science*, 2019, **365**, 367–369.
4 Y. Liu, B. Shi, Z. Liu, R. Gao, C. Huang, H. Alhumade, S. Wang, X. Qi and A. Lei, *J. Am. Chem. Soc.*, 2021, **143**, 20863–20872.
5 Y. Bai, Z. Wang, N. Qin, D. Ma, W. Fu, Z. Lu and X. Pan, *Angew. Chem., Int. Ed.*, 2023, **62**, e202303162.
6 R. Hilgers, S. Teng, A. Briš, A. Y. Pereverzev, P. White, J. J. Jansen and J. Roithová, *Angew. Chem., Int. Ed.*, 2022, **61**, e202205720.

7 D. Heller, B. Hagenhoff and C. Engelhard, *J. Vac. Sci. Technol., B:Nanotechnol. Microelectron.:Mater., Process., Meas., Phenom.*, 2016, **34**, 053401–053405.
8 K. Liu, S. Tang, T. Wu, S. Wang, M. Zou, H. Cong and A. Lei, *Nat. Commun.*, 2019, **10**, 639.
9 F. Cao, J. Kim and A. J. Bard, *J. Am. Chem. Soc.*, 2014, **136**, 18163–18169.
10 X. Liu, D. Yang, Z. Liu, Y. Wang, Y. Liu, S. Wang, P. Wang, H. Cong, Y.-H. Chen, L. Lu, X. Qi, H. Yi and A. Lei, *J. Am. Chem. Soc.*, 2023, **145**, 3175–3186.
11 S. den Hartog, S. Neukermans, M. Samanipour, H. Y. V. Ching, T. Breugelmans, A. Hubin and J. Ustarroz, *Electrochim. Acta*, 2022, **407**, 139704.
12 H. Li, D. Chao, B. Chen, X. Chen, C. Chuah, Y. Tang, Y. Jiao, M. Jaroniec and S.-Z. Qiao, *J. Am. Chem. Soc.*, 2020, **142**, 2012–2022.
13 M. Chen, D. Liu, L. Qiao, P. Zhou, J. Feng, K. W. Ng, Q. Liu, S. Wang and H. Pan, *Chem. Eng. J.*, 2023, **461**, 141939.
14 Y. Zhang, Y. Katayama, R. Tatara, L. Giordano, Y. Yu, D. Fraggedakis, J. G. Sun, F. Maglia, R. Jung, M. Z. Bazant and Y. Shao-Horn, *Energy Environ. Sci.*, 2020, **13**, 183–199.
15 F. Zaera, *Chem. Soc. Rev.*, 2014, **43**, 7624–7663.
16 S. Lin, S. Dikler, W. D. Blincoe, R. D. Ferguson, R. P. Sheridan, Z. Peng, D. V. Conway, K. Zawatzky, H. Wang, T. Cernak, I. W. Davies, D. A. DiRocco, H. Sheng, C. J. Welch and S. D. Dreher, *Science*, 2018, **361**, 6236.
17 A. Das, C. Weise, M. Polack, R. D. Urban, B. Krafft, S. Hasan, H. Westphal, R. Warias, S. Schmidt, T. Gulder and D. Belder, *J. Am. Chem. Soc.*, 2022, **144**, 10353–10360.
18 H. Cheng, T. Yang, M. Edwards, S. Tang, S. Xu and X. Yan, *J. Am. Chem. Soc.*, 2022, **144**, 1306–1312.
19 T. A. Brown, H. Chen and R. N. Zare, *J. Am. Chem. Soc.*, 2015, **137**, 7274–7277.
20 T. A. Brown, H. Chen and R. N. Zare, *Angew. Chem., Int. Ed.*, 2015, **54**, 11183–11185.
21 S. Bruckenstein and R. R. Gadde, *J. Am. Chem. Soc.*, 1971, **93**, 793–794.
22 O. Wolter and J. Heitbaum, *Ber. Bunsen-Ges.*, 1984, **88**, 2–6.
23 X. Xu, W. Lu and R. B. Cole, *Anal. Chem.*, 1996, **68**, 4244–4253.
24 F. Zhou and G. J. Van Berkel, *Anal. Chem.*, 1995, **67**, 3643–3649.
25 H. Cheng, S. Tang, T. Yang, S. Xu and X. Yan, *Angew. Chem., Int. Ed.*, 2020, **59**, 19862–19867.
26 R. G. Cooks, Z. Ouyang, Z. Takats and J. M. Wiseman, *Science*, 2006, **311**, 1566–1570.
27 T. H. Kuo, E. P. Dutkiewicz, J. Pei and C. C. Hsu, *Anal. Chem.*, 2020, **92**, 2353–2363.
28 Q. Wan, K. Chen, X. Dong, X. Ruan, H. Yi and S. Chen, *Angew. Chem., Int. Ed.*, 2023, **62**, e202306460.
29 J. Keller, H. Haase and M. Koch, *Anal. Bioanal. Chem.*, 2017, **409**, 4037–4045.
30 H. Yao, E. C. Sherer, M. Lu, J. Small, G. E. Martin, Y.-H. Lam, Q. Chen, R. Helmy, Y. Liu and H. Chen, *J. Org. Chem.*, 2022, **87**, 15011–15021.
31 V. Göldner, J. Fangmeyer and U. Karst, *Trends Anal. Chem.*, 2025, **185**, 118178.
32 W. Li, J. Sun, Y. Gao, Y. Zhang, J. Ouyang and N. Na, *Trends Anal. Chem.*, 2021, **135**, 116180.
33 K. Zhao, X. Jiang, X. Wu, H. Feng, X. Wang, Y. Wan, Z. Wang and N. Yan, *Chem. Soc. Rev.*, 2024, **53**, 6917–6959.
34 A. A. Abd-El-Latif, C. J. Bondue, S. Ernst, M. Hegemann, J. K. Kaul, M. Khodayari, E. Mostafa, A. Stefanova and H. Baltruschat, *Trends Anal. Chem.*, 2015, **70**, 4–13.
35 E. L. Clark, M. R. Singh, Y. Kwon and A. T. Bell, *Anal. Chem.*, 2015, **87**, 8013–8020.
36 E. L. Clark and A. T. Bell, *J. Am. Chem. Soc.*, 2018, **140**, 7012–7020.
37 B. Hasa, M. Jouny, B. H. Ko, B. Xu and F. Jiao, *Angew. Chem., Int. Ed.*, 2021, **60**, 3277–3282.
38 G. Tang, J. Zhang, S. Ma, J. Li, Z. Peng and W. Chen, *Chem. Soc. Rev.*, 2025, **54**, 7216–7251.
39 D. Cao, C. Tan and Y. Chen, *Nat. Commun.*, 2022, **13**, 4908.
40 J. Chen, E. Quattrocchi, F. Ciucci and Y. Chen, *Chem*, 2023, **9**, 2267–2281.
41 L. Pang, H. Li, X. Feng, Z. Zhao, C. Ouyang and Z. Peng, *ACS Energy Lett.*, 2024, **9**, 3587–3594.
42 T. Zhang, S. P. Palii, J. R. Eyler and A. Brajter-Toth, *Anal. Chem.*, 2002, **74**, 1097–1103.
43 J. Yang, L.-H. Ye, B. Wang, H. Zheng and J. Cao, *J. Sep. Sci.*, 2020, **43**, 3969–3981.
44 J. Xu, T. Zhu, K. Chingin, Y. Liu, H. Zhang and H. Chen, *Anal. Chem.*, 2018, **90**, 13832–13836.
45 M. Elsherbini and T. Wirth, *Acc. Chem. Res.*, 2019, **52**, 3287–3296.
46 Y. Mo, G. Rughoobur, A. M. K. Nambiar, K. Zhang and K. F. Jensen, *Angew. Chem., Int. Ed.*, 2020, **59**, 20890–20894.
47 F. T. G. van den Brink, L. Büter, M. Odijk, W. Olthuis, U. Karst and A. van den Berg, *Anal. Chem.*, 2015, **87**, 1527–1535.
48 T. Herl and F.-M. Matysik, *Anal. Chem.*, 2020, **92**, 6374–6381.
49 W. Nie, Q. Wan, J. Sun, M. Chen, M. Gao and S. Chen, *Nat. Commun.*, 2023, **14**, 6671.
50 S. Chen, Q. Wan and A. K. Badu-Tawiah, *Angew. Chem., Int. Ed.*, 2016, **55**, 9345–9349.
51 Q. Wan, S. Chen and A. K. Badu-Tawiah, *Chem. Sci.*, 2018, **9**, 5724–5729.
52 B. H. R. Gerroll, K. M. Kulesa, C. A. Ault and L. A. Baker, *ACS Meas. Sci. Au*, 2023, **3**, 371–379.
53 K. M. Kulesa, E. A. Hirtzel, V. T. Nguyen, D. P. Freitas, M. E. Edwards, X. Yan and L. A. Baker, *Anal. Chem.*, 2024, **96**, 8249–8253.
54 P. Khanipour, M. Loffler, A. M. Reichert, F. T. Haase, K. J. J. Mayrhofer and I. Katsounaros, *Angew. Chem., Int. Ed.*, 2019, **58**, 7273–7277.

55 F. F. J. de Kleijne, F. ter Braak, D. Piperoudis, P. H. Moons, S. J. Moons, H. Elferink, P. B. White and T. J. Boltje, *J. Am. Chem. Soc.*, 2023, **145**, 26190–26201.
56 M. Strach, V. Mantella, J. R. Pankhurst, P. Iyengar, A. Loiudice, S. Das, C. Corminboeuf, W. van Beek and R. Buonsanti, *J. Am. Chem. Soc.*, 2019, **141**, 16312–16322.
57 K. Z. Alzarieni, J. W. Marcum, E. Feng, T. Pourpoint and H. I. Kenttämaa, *J. Am. Soc. Mass Spectrom.*, 2023, **34**, 2381–2393.
58 Y. Li, M. Su, Y. Hou, Y. Zheng and Z. Zhang, *Chem. – Eur. J.*, 2025, **31**, e202404646.
59 J. Li, H. D. Dewald and H. Chen, *Anal. Chem.*, 2009, **81**, 9716–9722.
60 K. R. Brownell, C. C. McCrory, C. E. Chidsey, R. H. Perry, R. N. Zare and R. M. Waymouth, *J. Am. Chem. Soc.*, 2013, **135**, 14299–14305.
61 H. Cheng, X. Yan and R. N. Zare, *Anal. Chem.*, 2017, **89**, 3191–3198.
62 H. Zhang, K. Yu, N. Li, J. He, L. Qiao, M. Li, Y. Wang, D. Zhang, J. Jiang and R. N. Zare, *Analyst*, 2018, **143**, 4247–4250.
63 K. Yu, H. Zhang, J. He, R. N. Zare, Y. Wang, L. Li, N. Li, D. Zhang and J. Jiang, *Anal. Chem.*, 2018, **90**, 7154–7157.
64 J. Chen, X. Wang, X. Cui, Y. Li, Y. Feng and Z. Wei, *Angew. Chem., Int. Ed.*, 2023, **62**, e202219302.
65 S. Tang, H. Cheng and X. Yan, *Angew. Chem., Int. Ed.*, 2020, **59**, 209–214.
66 J. Bai, M. Bao, S. Wang, T. Wen, Y. Li, J. Zhang, T. Mei and Y. Guo, *Anal. Chim. Acta*, 2023, **1279**, 341794.
67 Y. Li, L. Zhu, X. Wu, Z. Zhang, R. Pu, Y. Zheng and Z. Zhang, *Angew. Chem., Int. Ed.*, 2024, **63**, e202318169.
68 R. Qiu, X. Zhang, H. Luo and Y. Shao, *Chem. Sci.*, 2016, **7**, 6684–6688.
69 C. Gu, X. Nie, J. Jiang, Z. Chen, Y. Dong, X. Zhang, J. Liu, Z. Yu, Z. Zhu, J. Liu, X. Liu and Y. Shao, *J. Am. Chem. Soc.*, 2019, **141**, 13212–13221.
70 J. Hu, N. Zhang, P.-K. Zhang, Y. Chen, X.-H. Xia, H.-Y. Chen and J.-J. Xu, *Angew. Chem., Int. Ed.*, 2020, **59**, 18244–18248.
71 C.-Y. Liu, Y. Chen and J. Hu, *Anal. Chem.*, 2024, **96**, 3354–3361.
72 R. Narayanan, P. Basuri, S. K. Jana, A. Mahendranath, S. Bose and T. Pradeep, *Analyst*, 2019, **144**, 5404–5412.
73 S. A. Miller and V. Bandarian, *J. Am. Chem. Soc.*, 2019, **141**, 11019–11026.
74 A. Koovakattil Surendran and J. Roithová, *Chem.:Methods*, 2024, **4**, e202400003.
75 X. Liu, J. Chen, Z. Wei, H. Yi and A. Lei, *Chem*, 2024, **10**, 2131–2146.
76 X. Cui, J. Chen, H. Yi and Z. Wei, *Anal. Chem.*, 2024, **96**, 17765–17772.
77 X. Zhang, W. Lu, C. Ma, T. Wang, J.-J. Zhu, R. N. Zare and Q. Min, *Chem. Sci.*, 2022, **13**, 6244–6253.
78 N. P. Lockyer, S. Aoyagi, J. S. Fletcher, I. S. Gilmore, P. A. W. van der Heide, K. L. Moore, B. J. Tyler and L.-T. Weng, *Nat. Rev. Methods Primers*, 2024, **4**, 32.
79 J.-G. Wang, R.-J. Yu, X. Hua and Y.-T. Long, *Chem. Soc. Rev.*, 2023, **52**, 2596–2616.
80 B. Liu, X.-Y. Yu, Z. Zhu, X. Hua, L. Yang and Z. Wang, *Lab Chip*, 2014, **14**, 855–859.
81 Z. Wang, Y. Zhang, B. Liu, K. Wu, S. Thevuthasan, D. R. Baer, Z. Zhu, X. Y. Yu and F. Wang, *Anal. Chem.*, 2017, **89**, 960–965.
82 J.-G. Wang, Y. Zhang, X. Yu, X. Hua, F. Wang, Y.-T. Long and Z. Zhu, *J. Phys. Chem. Lett.*, 2019, **10**, 251–258.
83 Y. Zhang, J.-G. Wang, X. Yu, D. R. Baer, Y. Zhao, L. Mao, F. Wang and Z. Zhu, *ACS Energy Lett.*, 2019, **4**, 215–221.
84 Y. Zhang, J. Tang, Z. Ni, Y. Zhao, F. Jia, Q. Luo, L. Mao, Z. Zhu and F. Wang, *J. Phys. Chem. Lett.*, 2021, **12**, 5279–5285.
85 C. Mu, T. Li, C. Zhan, Q. Fu, Y. Zhang, L. Zhang, F. Wang, Y. Zhang and X. Li, *Angew. Chem., Int. Ed.*, 2025, **64**, e202508456.
86 C. Kingston, M. D. Palkowitz, Y. Takahira, J. C. Vantourout, B. K. Peters, Y. Kawamata and P. S. Baran, *Acc. Chem. Res.*, 2020, **53**, 72–83.
87 S. B. Beil, D. Pollok and S. R. Waldvogel, *Angew. Chem., Int. Ed.*, 2021, **60**, 2–12.
88 T. H. Meyer, I. Choi, C. Tian and L. Ackermann, *Chem*, 2020, **6**, 2484–2496.
89 K. Chen, Q. Wan, S. Wei, W. Nie, S. Zhou and S. Chen, *Chem. – Eur. J.*, 2024, **30**, e202402215.
90 T. A. Brown, N. Hosseini-Nassab, H. Chen and R. N. Zare, *Chem. Sci.*, 2016, **7**, 329–332.
91 C. Liu, Q. Wang, B. E. Hivick, Y. Ai, P. A. Champagne, Y. Pan and H. Chen, *Anal. Chem.*, 2020, **92**, 15291–15296.
92 Q. Wang, Q. Wang, Y. Zhang, Y. M. Mohamed, C. Pacheco, N. Zheng, R. N. Zare and H. Chen, *Chem. Sci.*, 2020, **12**, 969–975.
93 J. He, N. Li, D. Zhang, G. Zheng, H. Zhang, K. Yu and J. Jiang, *Environ. Sci.: Water Res. Technol.*, 2020, **6**, 181–188.
94 J. Hu, T. Wang, H. Hao, W.-J. Zhang, Q. Yu, H. Gao, N. Zhang, Y. Chen, X.-H. Xia, H.-Y. Chen and J.-J. Xu, *Angew. Chem., Int. Ed.*, 2021, **60**, 18494–18496.
95 K. Liang, D. Zhang, Y. Su, L. Lu, J. Hu, Y. H. Chen, X. Zhang, A. Lei and H. Yi, *Chem. Sci.*, 2023, **14**, 4152–4157.
96 X. Zhang, Y. Zhang, M. Li, Q. Yan, W. Lu, J.-J. Zhu, X. Cheng and Q. Min, *Nat. Commun.*, 2025, **16**, 7452.
97 W. Li, J. Sun, Y. Wang, J. Qiao, L. He, J. Ouyang and N. Na, *Chem. Commun.*, 2021, **57**, 2955–2958.
98 Z. W. Seh, J. Kibsgaard, C. F. Dickens, I. Chorkendorff, J. K. Nørskov and T. F. Jaramillo, *Science*, 2017, **355**, 4998.
99 N.-T. Suen, S.-F. Hung, Q. Quan, N. Zhang, Y.-J. Xu and H. M. Chen, *Chem. Soc. Rev.*, 2017, **46**, 337–365.
100 G. Wang, J. Chen, Y. Ding, P. Cai, L. Yi, Y. Li, C. Tu, Y. Hou, Z. Wen and L. Dai, *Chem. Soc. Rev.*, 2021, **50**, 4993–5061.
101 W. Guo, X. Cao, D. Tan, B. Wulan, J. Ma and J. Zhang, *Angew. Chem., Int. Ed.*, 2024, **63**, e202401333.

102 K. Ye, T.-W. Jiang, H. D. Jung, P. Shen, S. M. Jang, Z. Weng, S. Back, W.-B. Cai and K. Jiang, *Nat. Commun.*, 2024, **15**, 9781.
103 G. Wen, B. Ren, X. Wang, D. Luo, H. Dou, Y. Zheng, R. Gao, J. Gostick, A. Yu and Z. Chen, *Nat. Energy*, 2022, **7**, 978–988.
104 Y. Wang, C. Wang, M. Li, Y. Yu and B. Zhang, *Chem. Soc. Rev.*, 2021, **50**, 6720–6733.
105 Y. Wang, W. Zhou, R. Jia, Y. Yu and B. Zhang, *Angew. Chem., Int. Ed.*, 2020, **59**, 5350–5354.
106 S. Han, H. Li, T. Li, F. Chen, R. Yang, Y. Yu and B. Zhang, *Nat. Catal.*, 2023, **6**, 402–414.
107 S. Zhang, J. Wu, M. Zheng, X. Jin, Z. Shen, Z. Li, Y. Wang, Q. Wang, X. Wang, H. Wei, J. Zhang, P. Wang, S. Zhang, L. Yu, L. Dong, Q. Zhu, H. Zhang and J. Lu, *Nat. Commun.*, 2023, **14**, 3634.
108 Q. Hu, W. Zhou, S. Qi, Q. Huo, X. Li, M. Lv, X. Chen, C. Feng, J. Yu, X. Chai, H. Yang and C. He, *Nat. Sustain.*, 2024, **7**, 442–451.
109 C. Lucky, L. Fuller and M. Schreier, *Catal. Sci. Technol.*, 2024, **14**, 353–361.
110 A. Bairagi, A. Y. Pereverzev, P. Tinnemans, E. A. Pidko and J. Roithová, *J. Am. Chem. Soc.*, 2024, **146**, 5480–5492.
111 X. Zhang, J. Zhan, H. Qin, J. Deng, J. Liu, M. Li, R. Cao and Y. Shao, *Chem. Sci.*, 2025, **16**, 5512–5517.
112 A. K. Surendran, A. Y. Pereverzev and J. Roithova, *J. Am. Chem. Soc.*, 2024, **146**, 15619–15626.
113 X. Zhang, Q. F. Chen, J. Deng, X. Xu, J. Zhan, H. Y. Du, Z. Yu, M. Li, M. T. Zhang and Y. Shao, *J. Am. Chem. Soc.*, 2022, **144**, 17748–17752.
114 J. M. Tarascon and M. Armand, *Nature*, 2001, **414**, 359–367.
115 Y. Chu, Y. Shen, F. Guo, X. Zhao, Q. Dong, Q. Zhang, W. Li, H. Chen, Z. Luo and L. Chen, *Electrochem. Energy Rev.*, 2020, **3**, 187–219.
116 Y. Yuan, K. Amine, J. Lu and R. Shahbazian-Yassar, *Nat. Commun.*, 2017, **8**, 15806.
117 Z. Zhu, Y. Zhou, P. Yan, R. S. Vemuri, W. Xu, R. Zhao, X. Wang, S. Thevuthasan, D. R. Baer and C.-M. Wang, *Nano Lett.*, 2015, **15**, 6170–6176.
118 Y. Zhang, M. Su, X. Yu, Y. Zhou, J. Wang, R. Cao, W. Xu, C. Wang, D. R. Baer, O. Borodin, K. Xu, Y. Wang, X.-L. Wang, Z. Xu, F. Wang and Z. Zhu, *Anal. Chem.*, 2018, **90**, 3341–3348.
119 Y. Zhang, Z.-Z. Shen, Y. Zhang, M. Niu, L. Dong, W.-P. Wang, D.-X. Xu, G. Li, L.-Y. Jiang, F. Wang, R. Wen, C. Yang, J.-Y. Liang, S. Xin and Y.-G. Guo, *Angew. Chem., Int. Ed.*, 2025, **64**, e202425491.
120 A. M. Tripathi, W.-N. Su and B. J. Hwang, *Chem. Soc. Rev.*, 2018, **47**, 736–851.
121 S. Kim, H.-S. Kim, B. Kim, Y.-J. Kim, J.-W. Jung and W.-H. Ryu, *Adv. Energy Mater.*, 2023, **13**, 2301983.
122 E. J. McShane, H. K. Bergstrom, P. J. Weddle, D. E. Brown, A. M. Colclasure and B. D. McCloskey, *ACS Energy Lett.*, 2022, **7**, 2734–2744.
123 K. Nishioka, K. Morimoto, T. Kusumoto, T. Harada, K. Kamiya, Y. Mukouyama and S. Nakanishi, *J. Am. Chem. Soc.*, 2021, **143**, 7394–7401.
124 Z. Yu, Y. Shao, L. Ma, C. Liu, C. Gu, J. Liu, P. He, M. Li, Z. Nie, Z. Peng and Y. Shao, *Adv. Mater.*, 2021, **34**, e2106618.
125 W. Miao, *Chem. Rev.*, 2008, **108**, 2506–2553.
126 M. M. Richter, *Chem. Rev.*, 2004, **104**, 3003–3036.
127 M. Hesari, K. N. Swanick, J. S. Lu, R. Whyte, S. Wang and Z. Ding, *J. Am. Chem. Soc.*, 2015, **137**, 11266–11269.
128 C. Ma, S. Wu, Y. Zhou, H.-F. Wei, J. Zhang, Z. Chen, J.-J. Zhu, Y. Lin and W. Zhu, *Angew. Chem., Int. Ed.*, 2021, **60**, 4907–4914.
129 A. Zanut, A. Fiorani, S. Canola, T. Saito, N. Ziebart, S. Rapino, S. Rebeccani, A. Barbon, T. Irie, H. P. Josel, F. Negri, M. Marcaccio, M. Windfuhr, K. Imai, G. Valenti and F. Paolucci, *Nat. Commun.*, 2020, **11**, 2668.
130 T. Han, C. Ma, L. Wang, Y. Cao, H. Y. Chen and J. J. Zhu, *Adv. Funct. Mater.*, 2022, **32**, 2200863.
131 W. Guo, H. Ding, C. Gu, Y. Liu, X. Jiang, B. Su and Y. Shao, *J. Am. Chem. Soc.*, 2018, **140**, 15904–15915.
132 J.-L. Liu, J.-Q. Zhang, Z.-L. Tang, Y. Zhuo, Y.-Q. Chai and R. Yuan, *Chem. Sci.*, 2019, **10**, 4497–4501.
133 Y. Wang, J. Ding, P. Zhou, J. Liu, Z. Qiao, K. Yu, J. Jiang and B. Su, *Angew. Chem., Int. Ed.*, 2023, **62**, e202216525.

